AN ABSTRACT OF THE THESIS OF

Paige Molzahn for the degree of Master of Science in Environmental Engineering presented on May 31, 2016.

Title: Batch and Continuous Flow Column Studies of Methane Consumption and Methanol Production by *Methylosinus Trichosporium* OB3b and *Methylomicrobium Buryatense* 5GB1 Immobilized in Ca-Alginate and Agarose Hydrogels

Abstract approved:

_____

Lewis Semprini

Two methanotrophs, *M. trichosporium* OB3b and *M. buryatense* 5GB1, were encapsulated using two methods to investigate the potential of methane conversion for biofuel production. Ca-alginate and low melt agarose were used to immobilize the methanotrophs for batch and continuous flow column testing. Varying protein concentrations, residence times, and immobilization methods were compared for methane consumption and product formation. An integrated Monod model was used in conjunction with batch experiments to derive kinetic parameters for each culture type, for suspended and immobilized forms. Suspended OB3b showed an average maximum substrate utilization rate, K_{max}, of 0.0089 mg CH_4/mg protein/min and a half saturation coefficient, K_s, of 2.3 mg CH_4/L. Suspended 5GB1 exhibited a K_{max} of 0.0093 mg CH_4/mg protein/min and K_s of 1.9 mg CH_4/L. OB3b immobilized in agarose and externally cross-linked alginate gel beads showed equivalent levels of

methane consumption when immobilization methods were directly compared and the K_s values were slightly higher indicating mass transfer limitations into the films.

Monod kinetic parameters were applied in conjunction with a biofilm diffusion-kinetics model developed by Rittmann and McCarty to simulate methane consumption in a constant mixed biofilm reactor (CMBR). The model provided a good fit to activity trends seen in continuous flow column tests such as higher extents of methane removal with respect to increasing biomass concentration.

OB3b was investigated for the direct production of methanol through chemical inhibition of the methanol dehydrogenase enzyme. Cyclopropane and cyclopropanol were used as inhibitors in batch and column reactors with immobilized cultures. Results showed initial concentrations of methanol production up to 0.12 mg methanol/L in a packed column reactor. Two consecutive cycles of inhibition were conducted to investigate re-inhibition of OB3b for long term methanol production. The two inhibition cycles produced equal levels of methanol and maintained constant levels of methane consumption, indicating OB3b can be effectively re-inhibited. Maximum levels of methanol conversion efficiency ranged from 13-17% for the batch reactor inhibited with cyclopropane exposure and 75-140% conversion efficiency for the continuous flow column inhibited directly with biologically produced cyclopropanol.

Batch and Continuous Flow Column Studies of Methane Consumption and Methanol
Production by *Methylosinus Trichosporium* OB3b and *Methylomicrobium
Buryatense* 5GB1 Immobilized In Ca-Alginate and Agarose Hydrogels

by
Paige Molzahn

A THESIS

submitted to

Oregon State University

in partial fulfillment of
the requirements for the
degree of

Master of Science

Presented May 31, 2016
Commencement June 2016

Master of Science thesis of <u>Paige Molzahn</u> presented on <u>May 31, 2016</u>

APPROVED:

_____

Major Professor, representing Environmental Engineering

_____

Head of the School of Chemical, Biological, and Environmental Engineering

_____

Dean of the Graduate School

I understand that my thesis will become part of the permanent collection of Oregon State University libraries. My signature below authorizes release of my thesis to any reader upon request.

_____

Paige Molzahn, Author

ACKNOWLEDGEMENTS

I would like to express my sincere gratitude to Dr. Lew Semprini for serving as my advisor and mentor throughout my time pursuing this degree. Lew has provided me with the guidance and leadership required for me to feel comfortable and confident in my research. He has given me the opportunity to work on a project I am passionate about, while guiding me through academic and personal growths. I am sincerely thankful for all that he has done to help me through this process. I would also like to thank the ARPA-E program for funding this and many other interesting and innovative research opportunities.

I would also like to thank my friends from the lab; Dr. Anne Taylor, Dr. Mohammad Azizian, Clint Montgomery, Monique LaJeunesse, and many more. At one point or another all of these wonderful people provided me with support in the lab. Whether it be technical help with lab equipment, running hours of experiments, or giving me the training required to be successful in the lab, this group was always there to support me when needed.

I would like to express my sincere gratitude to the members of my committee; Dr. Mark Dolan, Dr. Karl Schilke, and Dr. Jack Istok. Mark and Karl have provided me with guidance and advice through the entirety of my graduate school experience. I am so thankful for the opportunity to work with them directly on this research project, and have enjoyed the many hours of meetings we have all endured to make this project a success.

Finally, I would like to thank my friends and family for supporting me in and out of my academic pursuits. My parents, Bill and Susan, and brother, Doug, have provided me with the encouragement and confidence to pursue my dreams, and also some hilarious entertainment along the way! Thank you to my roommates and closest friends who have endured many hours of discussions and provided incredible advice when I am in need of a quick pep talk. Thank you again, to everyone who has helped me through the past two years of research, I sincerely appreciate it.

TABLE OF CONTENTS (Continued)

LIST OF FIGURES

LIST OF FIGURES (Continued)

LIST OF APPENDIX FIGURES

LIST OF TABLES

LIST OF APPENDIX TABLES

Nomenclature

a………………specific surface area (cm^{-1})

CMBR………...constant mixed biofilm reactor

C_L……………...liquid substrate concentration (mg/mL)

D, D_f…………...substrate diffusion coefficient (cm^2/s)

ETO…………....ethylene oxide

f……………..ratio comparing actual flux to theoretical values

GDL …………..glucono-δ-lactone, compound used for internal gelation

H_{cc} ………..……Henry's Law constant (dimensionless)

hV ……………...liquid volume in reactor, used in CMBR model development (mL)

J_{deep}……………..substrate flux into a biofilm defined as deep $(mg/cm^2/s)$

J_{ss}………………substrate flux into a biofilm at steady state $(mg/cm^2/s)$

kD………………measurement of atomic mass (kilodalton)

K_{max}……………..maximum substrate utilization rate (mg CH_4/mg protein/min)

$K_{max,app}$…………..maximum substrate utilization rate (mg CH_4/mg protein/min)

K_s………………..half saturation coefficient from Monod equation (mg/mL)

L………………..depth of film (cm)

MDH……………methanol dehydrogenase enzyme

MMO……………methane monooxygenase enzyme

NMS……………nitrate minerals salt

OB3b……………name for methanotrophic culture *Methylosinus trichosporium*

Q………………..flow rate (mL/min)

S………………..substrate concentration (mg/mL)

SSE……………sum of squared errors

t…………………time (min)

V…………………reactor volume (mL)

V_G………………..volume of gas (mL)

V_L………………..volume of liquid (mL)

V_{max}………………maximum substrate utilization rate (mg CH_4/mg protein/min)

X_a, X_f……………..biomass concentration (mg protein/mL bead)

Y…………………cell yield coefficient (mg protein/mg CH_4 consumed)

z…………………thickness of biofilm (cm)

5GB1……………..name for methanotrophic culture *Methylomicrobium buryatense*

CHAPTER 1
INTRODUCTION

Methane is a harmful and prominent greenhouse gas, second only to carbon dioxide (Myhre & Shindell, 2013). It is commonly produced as a byproduct in natural gas processes, petroleum systems, enteric fermentation, and landfills (Hwang et al., 2014). Atmospheric concentrations of methane are rapidly increasing and current methods of methane removal, such as flaring and venting, are only contributing to the environmental problem (Myhre & Shindell, 2013) (Gilman et al., 2015). Storing and shipping the gas is not a viable removal option as it is dangerous and expensive, therefore, a new method of methane conversion is required.

An alternative option for methane removal is a gas-to-liquid conversion via the Fischer-Tropsch process. This process converts mixtures of carbon and hydrogen to liquid hydrocarbons through chemical reactions. Current approaches for this method require numerous stages and processes that include pressure and heat changes, decreasing economic feasibility. To avoid these issues, investigations for improvement of natural microbial bioconversion are being conducted (Haynes & Gonzalez, 2014). Microbes have the natural capability to perform this bioconversion and recent developments in synthetic biology are improving process viability. Potential obstacles associated with this process are naturally slow microbial rates and mass transfer limitations. These concerns can be eliminated by immobilizing enhanced versions of the cultures in a hydrogel in a high mass transfer reactor.

A bio-lamina plate (BLP) reactor is a micro-reactor being developed for this purpose. The BLP reactor will contain a thin film of immobilized cultures in a

hydrogel with liquid and gas bubbles flowing over the film. The gas bubbles will be converted to product in the liquid phase via enhanced microbial conversion. Methane utilization by way of the methane monooxygenase (MMO) enzyme, found in methanotrophic bacteria, is a practical option for this enhanced bioconversion (Kaluzhnaya & Khmelenina, 2001; Lee et al., 2006; Lee et al., 2004; Gonzalez & Conrado, 2014). Understanding long term behavior and activity in immobilized hydrogels is a vital component in pursuing the gas-to-liquid bioconversion process.

Two strains under investigation for the utilization are *Methylomicrobium buryatense* 5GB1 and *Methylosinus trichosporium* OB3b. 5GB1 is a methanotroph isolated from a soda lake in Eastern Russia and can withstand high pH and salt content. This bacteria has the ability to grow rapidly with a reported doubling time of 2.9 hours (Gilman et al., 2015). OB3b prefers a lower pH and salt content, but is equally capable of high methane oxidation rates (Eller et al., 2001; Furuto et al., 1999). Utilizing these two strains, 5GB1 and OB3b, for the conversion of methane provides a possibility for future methane removal processes.

Each methanotroph follows an enzyme pathway that converts methane to methanol, and then to formaldehyde, formate, and finally carbon dioxide (Lee et al., 2004; Murrell et al., 2008; Jiang et al., 2010). The two enzymes of interest are methane monooxygenase (MMO) and methanol dehydrogenase (MDH). Methanotrophs can be altered chemically or genetically for the production of a usable product, such as biofuels or specialty chemicals. OB3b can be chemically inhibited to decrease the activity of the methanol dehydrogenase enzyme, allowing methanol to accumulate as a usable product (Lee et al., 2004). Multiple methods of inhibition have

been investigated, but the use of cyclopropane and cyclopropanol have been proven to be most effective (Lee et al., 2004). 5GB1 is currently being investigated for genetic modification and enhancement of the enzyme pathway to produce different usable products including 2,3-butanediol from research conducted at University of Washington (Gilman et al., 2015)

An effective method of testing these methanotrophs for product formations is through the use of immobilization in gel beads and films. Immobilization in alginate and agarose provide benefits such as holding the bacteria in place, simple removal of free flowing products, and continuous operating conditions (Aksu et al., 1998) (Kourkoutas et al., 2004). Alginate and agarose are commonly used immobilization methods because they retain a significant amount of activity and can maintain an environment compatible with culture needs (Li et al., 1996; Narayanan et al., 2006). Immobilizing the cultures and placing them in batch, column or thin film reactors allows simple investigations of substrate utilization rates, biomass dependencies, and residence time effects on overall activity (Lee et al., 2004; Tsezos & Deutschmann, 1990).

Batch and plug flow reactor models have been developed for comparing experimental behaviors to theory. Modeling of the reactors with immobilized cultures includes the incorporation of flux into the immobilized form, substrate utilization, and mass balances dependent on reactor type. Accounting for substrate diffusion into these immobilized forms can be difficult, and generally a fraction of the limiting substrate's diffusion coefficient into water is used (Kostov et al., 2012; Tsezos & Deutschmann, 1992). Applying models that align with experimental findings are

beneficial for determining the effects of immobilization on activity (Tsezos & Deutschmann, 1992; Rittmann & McCarty, 2001). Rittmann and McCarty have fully developed models for biofilms in reactors for multiple conditions that align very well with experimental data (Rittmann & McCarty, 2001). These models are combined with Monod kinetic parameters from batch testing to get a full understanding of the behaviors in immobilized cultures (Smith et al., 1998).

Batch and packed column experiments were conducted to investigate the effects of immobilization, biomass concentrations and residence times within the packed column. 5GB1 and OB3b were immobilized in agarose and alginate, respectively, and placed in batch vials or packed into a small up-flow single phase column. Cell protein ranges were investigated between 0.6 and 18 mg biomass/mL of beads and residence times between 1 and 8 minutes for methane consumption and methanol production testing. Models were applied to these experimental results to predict column behaviors and gain a better understanding of limits on protein concentrations.

This thesis will discuss the investigation of three main objectives, each chapter will be divided into the subgroups shown below.

1. Demonstrate OB3b and 5GB1 can be immobilized in alginate or agarose and achieve activities similar to suspended cells. Results of batch tests can be simulated using an integrated Monod model.

2. Show biofilm continuous flow column tests can be simulated with a model developed for constantly mixed biofilm reactors with a flux incorporating substrate diffusion and utilization.

3. Determine whether externally cross-linked or internally gelated Ca-alginate gels were more effective in maintaining activity in OB3b.

4. Demonstrate methanol production in sequencing batch reactors and a continuous flow reactor could be achieved through the inhibition of the OB3b MDH enzyme using cyclopropane and cyclopropanol.

CHAPTER 2
LITERATURE REVIEW

2.1 Methane problems in atmosphere

      Methane is the second most prominent greenhouse gas to carbon dioxide and

has the potential to trap around 30 times more heat than carbon dioxide, making it

much more harmful (Myhre & Shindell, 2013). This gas is currently being produced

through natural and industrial processes such as anaerobic digestion, landfill sites,

petroleum systems, enteric fermentation, and natural gas processes (Hwang et al.,

2014; "Overview of Greenhouse Gases," 2016). There is growing concern over this

greenhouse gas due to rapidly increasing environmental concentrations. In 2011,

concentrations reached 1800 parts per billion (ppb) and are constantly increasing

(Myhre & Shindell, 2013). Storing and shipping methane is not an economically

feasible removal option, so current removal practices consist of flaring and venting

into the atmosphere. These processes continue to harm the environment (Gilman et

al., 2015).

      Significant dangers and strict regulations come with the storage and

transportation of methane, so an onsite solution for effluent methane removal is

greatly needed. The EPA has plans to tighten regulations on hazardous emissions

contributing to air pollution in 2016, which would force large scale operations to find

alternative methods of methane removal ("Overview of Greenhouse Gases," 2016).

One of the processes currently being developed for methane removal is biological

methane conversion. This development will potentially provide a viable option for

converting methane into a usable biofuel or specialty chemical through use of

methanotrophic bacteria (Haynes & Gonzalez, 2014; Duan et al., 2011; Kaluzhnaya

& Khmelenina, 2001; Han et al., 2013). The U.S. Department of Energy's Advanced

Research Projects Agency-Energy (ARPA-E) is currently funding 15 projects across

9 states with a total of $34 million for research working towards the conversion of

methane to liquid fuels for the REMOTE program (Reducing Emissions Using

Methanotrophic Organisms for Transportation Energy).

2.2 History of methanotrophs

2.2.1.   Basic properties

Methane can be oxidized rapidly through utilization of the MMO enzyme

found in methanotrophic bacteria. The methane oxidation pathway shown in *Figure 1*

takes methane through to carbon dioxide with intermediates of methanol,

formaldehyde, and formate. Methane is oxidized by the MMO enzyme to methanol,

and methanol is converted by the MDH enzyme to formaldehyde. Half of the

formaldehyde produced is assimilated into cell carbon and the remaining half is

converted into carbon dioxide to provide reducing power needed for the initial

oxidation step (Murrell et al., 2008).
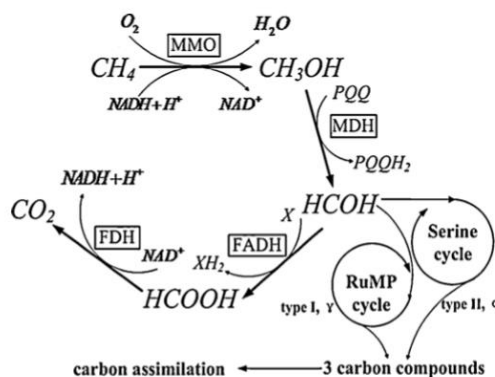
Figure 1. Enzyme pathway for methanotrophs. Displays conversion of methane to carbon dioxide. (Jiang et al., 2010).

Methanotrophic bacteria have the unique ability to grow using methane as their sole source of carbon and energy (Lee et al., 2006) (Lee et al., 2004), making it an exciting option for biofuel production, especially when comparing it to the energy intensive Fischer-Tropsch process. Microbes can effectively transform methane at low temperatures, eliminating high cost factors from Fischer-Tropsch transformations. There are two types of methanotrophic bacteria, Type I and Type II. The main differences are pathways utilized for formaldehyde assimilation, grouping of intracytoplasmic membranes, and the chain lengths of their fatty acids (16 and 18 carbons). Although there are differences in the types, they are both capable of the oxidation of methane through the MMO enzyme.

Methanotrophic bacteria are easy to grow, have wide ranges of substrate possibilities, are multifunctional, and can be genetically manipulated. All of these characteristics make methanotrophs a potential option for biofuel production at industrial scales (Hanson & Hanson, 1996).

2.2.2. *Methanotroph uses*

Methanotroph pathways have been of interest for processes related to biotransformation, bioremediation, and single-cell protein production (Murrell et al., 2008). These cultures have the ability to be immobilized in gel beads or films and retain significant levels of activity. For example, the methanotroph *Methylocystis Sp.* was immobilized in a fluidized-bed using gel beads for the removal of trichloroethylene (TCE) from ground water (Shimomura et al., 1997; Uchiyama, et al., 1995). The study determined that the methanotroph had the ability to remove the TCE, however it required a period of cell recovery every other day to maintain high

levels of removal (Shimomura et al., 1997). A similar approach was taken for the removal of chlorinated solvents, however the methanotrophic bacteria was grown into a natural biofilm and was attached to pellets which were placed in a two-phase reactor (Speitel Jr & McLay, 1993). The natural biofilms were able to support a reasonable level of methane and chlorinated solvent removal through cometabolism, but the technology was decidedly economically infeasible (Speitel Jr & McLay, 1993).

2.2.3. Type I

Type I methanotrophs belong to the gamma-proteobacteria Methylococcaceae family and are a gram negative aerobe (Jiang et al., 2010). Type I methanotrophs utilize the RuMP pathway for formaldehyde assimilation. A majority of methanotroph genera are members of this Type I family (Eller et al., 2001), examples being *Methylobacter, Methylomicrobium, Methylomonas,* and *Methylococcus* (Jiang et al., 2010). *Methylomicrobium buryatense* 5GB1 is a Type I methanotroph newly under investigation for the conversion of methane to usable product (Gilman et al., 2015).

5GB1 is a robust bacteria initially isolated from a soda lake in Eastern Russia. It grows in high pH (9.5) and high salt conditions and has the ability to grow rapidly, with a doubling time of 2.9 hours (Gilman et al., 2015). The high salt and pH conditions are desirable for large industrial scale processes because cultures will be less susceptible to outside contaminations. Carbon dioxide is the final product in the pathway which is not desirable, but 5GB1 has the potential to undergo genetic modification for accumulation of a usable product. Work is currently being conducted

in conjunction with this project by University of Washington and Rice University on the genetic modification of the strain.

2.2.4. *Type II*

Type II methanotrophs belong to the alpha-proteobacteria Methylocystaceae family (Eller et al., 2001). Type II methanotrophs include *Methylocystis, Methylosinus, Methylocapsa,* and *Methylocella* (Jiang et al., 2010). The serine pathway is utilized for formaldehyde assimilation and these bacteria are also gram negative aerobes. Type II methanotrophs are resilient to harsh conditions and can maintain high levels of activity in various environments. *Methylosinus trichosporium* OB3b is a Type II methanotroph that has been closely investigated for bioremediation, especially of chlorinated solvents (Fox et al., 1990). OB3b requires a neutral pH (7.5) and grows on a nitrate mineral salts (NMS) medium commonly used for bacterial growth (Furuto et al., 1999). OB3b bacteria has the ability to express both particulate and soluble forms of the MMO enzyme, depending on concentrations of copper present in growth media.

2.2.5. *Methane monooxygenase enzyme*

Methanotrophs grown on single carbon compounds have the ability to express two different forms of the MMO enzyme, soluble and particulate. The sMMO enzyme is in the soluble cytoplasmic form and the pMMO is in the particulate membrane form. Components of the sMMO enzyme include a hydroxylase, reductase, and a regulatory protein required for activity and it is a non-heme enzyme containing iron (Murrell et al., 2008). sMMO has the potential to transform a broad range of compounds such as carbon monoxide, ethane, propane, and butane, making

it more accessible for industrial applications (Lee et al., 2006) (Jiang et al., 2010). However, both expressions of the enzymes are capable of effective methane consumption in aerobic conditions. When copper is present at concentrations around 5 µM, pMMO will be expressed (Lee et al., 2004).

The pMMO enzyme is contained in nearly all methanotrophs and is comprised of three subunits called pmoA, pmoB, and pmoC (Hakemian & Rosenzweig, 2007). Kinetic comparisons of the pMMO and sMMO activity for OB3b were reported in Lee et al., 2006. OB3b expressing pMMO had a maximum methane consumption rate (K_{max}) of 82 nmol/min/mg protein and a half saturation coefficient (K_s) of 8.3 µM. sMMO had a K_{max} 726 nmol/min/mg and K_s of 92 µM. With the wide range of substrate potential and higher expected rates, the sMMO enzyme is a more viable option for high rate product formation. sMMO has the ability to catalyze the hydroxylation of alkenes in almost all forms including terminal, internal, substituted and branch-chain (Patel et al., 1982) (Colby et al., 1977).

2.2.6. *Methanol dehydrogenase enzyme*

The second enzyme in the methanotroph pathway is the MDH enzyme catalyzing the oxidation from methanol to formaldehyde (*Figure 2*) (Lee et al., 2004). MDH is an extensively studied enzyme characterized as a pyrroloquinoline quinone dependent quinoprotein (Kalyuzhnaya et al., 2008) (Anthony & Williams, 2003). The MDH enzyme has the ability to oxidize a large range of substrates (primary alcohols), but has the highest affinity for methanol (Kalyuzhnaya et al., 2008). MDH can be inhibited by various compounds to prevent methanol conversion, allowing it to

accumulate as the main product. This chemical inhibition process will be discussed in

further detail in the following section.
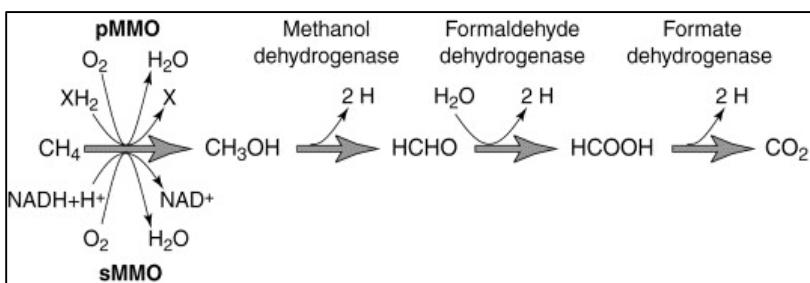
Figure 2. Enzyme pathway for OB3b. Displays the expression of both pMMO and sMMO as well as the conversion of methanol by the MDH enzyme. (Murrell et al., 2008).

2.2.7. *Chemical inhibition of MDH*

One possible function of methanotrophic bacteria is conversion of a natural

gas to a biofuel. This process can be completed through genetic modification or

chemical inhibition. Chemically inhibiting the MDH enzyme allows methane to be

consumed and the methanol to be produced and then accumulate. Inhibition is a

process where a molecule binds to an enzyme to decrease activity of that enzyme.

There are multiple mechanisms for this inhibition including complete blockage of the

substrate entering the active site and hindering the enzyme from catalyzing the

reaction. Chemical inhibition of MDH in OB3b has been investigated for product

formation. Both organic and inorganic compounds have been used as inhibitors,

examples are high concentrations of phosphate or low concentrations of cyclopropane

and cyclopropanol (Lee et al., 2004) (Shimoda & Okura, 1990). Although all of these

compounds are capable of inhibition, cyclopropanol is the most effective. Difficulties

that come with the storage and synthesis of cyclopropanol include instability of

compound over significant periods of time (Lee et al., 2004).

Optimal conditions for methanol production by OB3b and cyclopropanol inhibition achieved in Lee et al., 2004 were at temperature of 25°C, 20mM sodium formate concentration, and a cell density of 0.6 mg dry cell/mL. With these optimal conditions OB3b accumulated a total of 7.7 mM methanol over 36 hours in a batch reactor (Lee et al., 2004). Formate presence is of interest because it acts as an electron donor and has the potential to increase methanol production levels. Investigations are ongoing for the modification of MDH to eventually allow the accumulation of the methanol without using chemical inhibition techniques.

Issues associated with production of methanol are high methanol concentrations inhibiting MMO activity and that accumulated methanol can be continually oxidized by the uninhibited MMO enzyme (decreasing concentrations of product) (Furuto et al., 1999). For this reason a batch reactor is not a viable option for methanol production. In a study, for continuous production of methanol in a sequencing batch reactor, it was found that increasing the levels of methane entering the system did not provide any increased methanol accumulation (Furuto et al., 1999).

2.3 Immobilization

2.3.1. Immobilization background

Investigation of simple substrate conversion and contaminant removal commonly use methods of immobilizing bacteria in alginate or agarose gels. Cultures can be immobilized depending on their environmental requirements including pH, salt content, and temperature. The immobilization process provides many benefits, as presented by Kourkoutas et al., 2004. The benefits are prolonged activity, higher cell densities, increased substrate uptake and yield, continuous processing, low-

temperature capabilities, simple product recovery, regeneration and reuse of microbe, lowered risk of contamination, and ability to use micro-reactors. A review of the issues was also presented, including mass transfer limitations through diffusion, disturbances in growth, surface tension, osmotic pressure effects, reduced water activity, cell-to-cell communication, changes in cell morphology, altered membrane permeability, and media component availability (Kourkoutas et al., 2004; Aksu et al., 1998). The negatives are outweighed by the potential positives for immobilized bioconversion.

Immobilization is frequently used for removal of heavy metal ions from industrial and natural waste water (Tsezos & Deutschmann, 1990; Aksu et al., 1998; Canizares et al., 1993). A packed column comparison of Ca-alginate, agarose, and a green algae was conducted to understand the effects of flow rate and inlet concentrations on heavy metal removal. Immobilization allowed for a more economically feasible option than current metal removal methods (Tsezos & Deutschmann, 1990; Lee et al., 2004).

The pharmaceutical industry has extensively studied effects of various immobilization methods and their diffusion properties. Another use for immobilization is in the food industry, specifically alcohol production. Investigations are ongoing for immobilization of yeast for improved wine production (Kourkoutas et al., 2004). Polymeric materials are commonly used for this immobilization, including alginate, cellulose, carrageenan, agar, pectic acid, and chitosan (Kourkoutas et al., 2004; Plessas et al., 2007; Obuekwe & Al-Muttawa, 2001). Investigation of

immobilization effects on microbes requires evaluation of microbial activity in suspended and immobilized cells (Li et al., 1996; Narayanan et al., 2006).

2.3.2. Alginate review

2.3.2. i. External cross linking

Alginate hydrogels have been selected as a viable method of immobilization for OB3b because it supports media requirements and can effectively be included in gel formulations. Alginate is a polysaccharide with a linear 1,4 linked copolymer of beta-D-mannuronic acid (Chan et al., 2002). Alginate gels are produced by an extrusion process using calcium as a cross-linking agent. Alginate is water soluble and when exposed to calcium ions cross linking occurs (Steinbüchel, 2005). Helping to create the cross linking, calcium ions displace two of the sodium ions and the alginate contains hydroxyl groups that can be oriented to the added cations, as shown in *Figure 3,*. Effects of varying crosslinking conditions, polymer concentration, and direction of diffusion on transport in both alginate and agarose were investigated by Li et al., 1996. In general, the 1.5-3% alginate gels offered transport resistance for solutes in the molecular weight range 44-155 kD, lowering their diffusion rates from 10- to 100-fold as compared to their diffusion in water (Li et al., 1996).
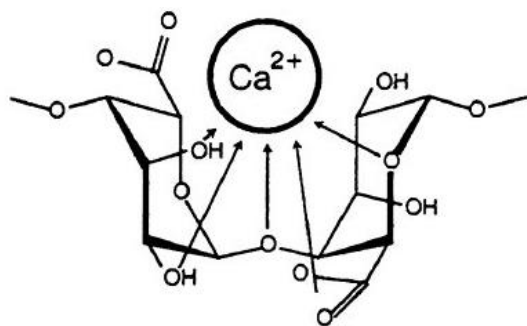
Figure 3. A calcium ion linking to two hydroxyl groups after the displacement of the sodium ion (Steinbüchel, 2005).

Dropping mixtures of alginate into calcium solutions forces cross-linking to occur on the exterior of the alginate creating a hydrogel bead. Thin film geometries can also be formed by spreading a thin layer of alginate and exposing it to the calcium solution (Chan et al., 2002). An example of an alginate hydrogel bead is shown in *Figure 4*.
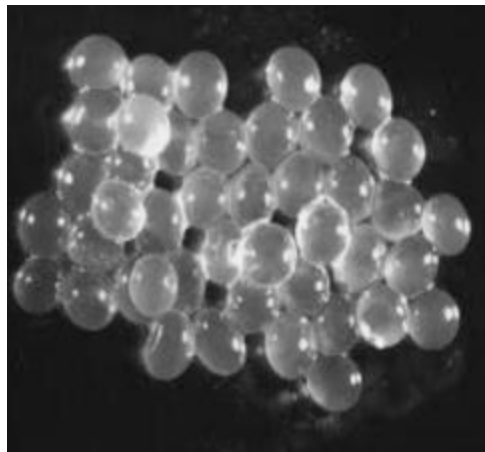
Figure 4. Image of example alginate beads. (Gouin, 2004).

2.3.3. ii.   Internal gelation

As previously mentioned, alginate can be cross-linked externally using calcium salts, however beads can also be formed through internal gelation. Internal gelation benefits include use of less calcium salt and increased control over morphology (Chan et al., 2002). Calcium can be added to alginate at varying concentrations to increase the hardness of the microspheres. This requires glucono-delta-lactone (GDL) as a slow acidifier,. The GDL is a white powder that is soluble in water and when added to an aqueous solution it hydrolyses to gluconic acid in the solidification process. Alginate and GDL have been used together in the food industry for effective gelation of alginate (Kohyama et al., 1992). Internal gelation provides a simpler method for creating geometries, with more control.

2.3.3. Agarose review

Agarose is second common form of immobilization. Alginate and agarose can generally be used for similar purposes, however each has different temperature and pH requirements. Agarose is a marine polysaccharide that can form gels through the creation of agarose chain bundles linked by hydrogen bonds. The gels have the ability to hold water and culture suspensions and can withstand high pH and salt concentration. Li et al. (1996) determined 2-4 wt% agarose gels offered little transport resistance for solutes up to 150 kD, therefore agarose provides less transfer resistance for substrates entering the film than alginate (providing an advantage when working towards high activity requirements) (Li et al., 1996). Agarose is mixed and heated beyond the melting point and once cooling begins, cultures can be added to the mixture before complete solidification.

2.4 Packed column design and modeling

2.4.1. Current uses for packed column

Industries often use packed column designs at the bench scale to predict process scale-up performance. Packed columns containing immobilized cultures have been used for processes including bioremediation, medical applications, and within the food industry. Packed columns are a viable option because they provide a low manufacturing and operating cost while still maintaining high rates of activity and production (Chan et al., 2002). Optimization of column diameter, height, total volume, bed volume, void volume, and packing method is vital for increased reactor performance. Packing of a column depends on particle geometry, size, volume and

content. Determining which parameters are most influential for a given system can be completed using a sensitivity analysis (Tsezos & Deutschmann, 1992).

Columns packed with immobilized cultures are generally used for small scale testing of metal removal, water treatment, and alcohol production. Specific process engineering advantages to running an experiment in a packed column format are the simple scaling opportunities and high yield operations (high degrees of turnover in a one step process). A packed column is modeled very simply through plug-flow behavior or constant mixed batch reactors in series (Aksu et al., 1998).

2.4.2. *Modeling approaches*

2.4.2. i. *Integrated Monod for batch reactor*

When evaluating microbial performances, batch and continuous flow reactors can be used. Batch reactors are useful when investigating kinetics and for directly comparing rates. Monod and Michaelis-Menten equations are often used when evaluating batch kinetic tests. The Monod equation for substrate reaction rate of a bacterial culture is shown in *Equation 1*.

$$-\frac{dC_L}{dt} = \frac{K_{max}X_a C_L}{(K_s + C_L)} \tag{1}$$

This equation can be integrated and manipulated to fit substrate consumption data versus time for changing protein concentrations (Smith et al., 1998). *Equation 2* represents growth of bacteria within a system with respect to substrate utilization. *Equation 3,* is the integrated Monod equation solved for time.

$$X_a = X_{a,0} + Y(C_{L,0} - C_L) \tag{2}$$

$$t = \frac{1}{K_{max}} \left\{ \begin{array}{c} \frac{K_S}{X_{a0}+YC_{L0}}\ln(X_{a0} + Y(C_{L0} - C_L)) + \frac{K_S}{X_{a0}+YC_{L0}}\ln\left(\frac{C_{L0}}{X_{a0}C_L}\right)\dots \\ \dots + \frac{1}{Y}\ln(X_{a0} + Y(C_{L0} - YC_L)) - \frac{1}{Y}\ln(X_{a0}) \end{array} \right\} \tag{3}$$

With t being time, K_{max} as the maximum substrate utilization rate, K_s as the

half saturation coefficient, $X_{a,}$ as the protein concentration, Y as cell yield coefficient,

and C_L as substrate concentration in liquid phase. The model is used in conjunction

with substrate consumption data for kinetic parameter estimations.

2.4.2. ii.   *Modeling of CMBRs in series*

A completely mixed biofilm reactor (CMBR) model can be applied to

experimental reactor data to verify system parameters. Mass balances, diffusion

equations, and rate kinetics can be combined and applied to a CMBR model for

performance comparisons. Parameters significantly impacting CMBR performance

include influent flow rate, reactor volume, void fraction, specific surface area,

biomass accumulation, and effluent flow rate (Rittmann & McCarty, 2001). A basic

CMBR schematic from Rittmann and McCarty in *Environmental Biotechnology* is

shown in *Figure 5* with relevant parameters in the following image.
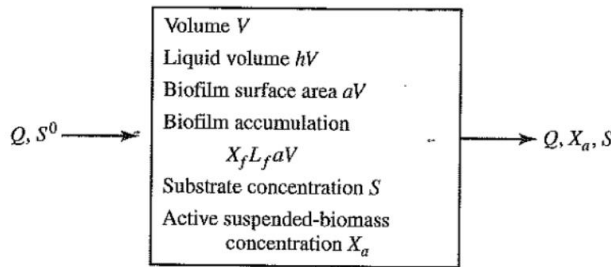
Figure 5. Example of the parameters of interest when modeling a reaction-diffusion into an active biofilm. (Rittmann & McCarty, 2001).

A steady state mass balance on a substrate in a CMBR is shown in *Equation 4* (Rittmann & McCarty, 2001). This balance is specifically derived for a biofilm within a CMBR with substrate diffusing and reacting in the film.

$$0 = Q(S^0 - S) - J_{ss}aV \tag{4}$$

Q is the flow rate, a is the specific surface area of the film, V is reactor volume, S is the substrate concentration, and J_{ss} is the substrate flux into the biofilm at steady state. Calculation of the flux into the biofilm is discussed in greater detail in the following section.

2.4.2. iii. Substrate utilization and diffusion

Diffusion and substrate utilization play a role in microbial biofilm systems and can greatly effect performance. Commonly, a biofilm reactor has two or three phases; biofilm, liquid, and sometimes a gas phase (Chang & Rittmann, 1987). Liquid and gas phases carry substrate to be diffused and converted in a biofilm. Diffusion coefficients used in immobilized systems are lowered to account for the limited diffusion into the biofilm. The lowered coefficient is due to the interactions with the polymers, particles, and cells preventing easy diffusion.

A model derived by Rittman and McCarty incorporates the steady state balance across each reactor (*Equation 4*), bacterial kinetic within a biofilm, and diffusions properties into a biofilm. The model is based on Fick's laws of diffusion and Monod kinetics (Usha et al., 2012). The main assumptions for the derivation of the model applied are represented in the following boundary conditions:

- Substrate concentrations at the biofilm and media interface are equal, the boundary condition at the liquid-film interface is shown in *Equation 5* below:

$$J = \frac{D}{L}(S - S_s) = D_f \left.\frac{dS_f}{dz}\right|_{z=0} = D \left.\frac{dS}{dz}\right|_{z=0} \tag{5}$$

- Substrate flux at film attachment is zero, *Equation 6*.

$$\left.\frac{dS_f}{dz}\right|_{z=L_f} = 0 \tag{6}$$

Substrate utilization and diffusion into the biofilm at a steady state are described in *Equation 7*. The first term represents substrate diffusion and the second represents substrate utilization.

$$0 = D_f \frac{d^2 S_f}{dz^2} - \frac{K_{max}X_f S_f}{K_s + S_f} \tag{7}$$

Equation 8 is the general solution for steady state flux into a biofilm. This equation is the analytical solution for *Equation 7* using the previously listed boundary conditions (*Equations 5* and *6*). Concentrations at the interface (S_s and S_f) must be known or assumed for this equation to be valid.

$$J_{deep} = \left[2K_{max}X_f D_f \left(S_s + K_s ln \left(\frac{K_s}{K_s + S_s} \right) \right) \right]^{1/2} \tag{8}$$

J_{deep} is the steady state flux into biofilm, D_f is the molecular diffusion coefficient of substrate into the film (80% of the diffusion coefficient of methane into water), K_s is the half saturation, and K_{max} is the maximum substrate utilization rate. This flux equation is used in conjunction with the steady state mass balance on the CMBR (*Equation 4*) to solve for effluent substrate concentrations for a set of parameters.

If experimental flux values vary from theory it is possible to use the following equation to convert from J_{deep} to J_{ss}, as demonstrated in *Equation 9*.

$$J_{ss} = fJ_{deep} \tag{9}$$

With f being the ratio expressing how much actual flux is reduced because the steady state film is not deep. The determination of f requires fits from numerical solutions, described in Saez and Rittmann (1992). The equations combined with a pseudo-analytical solution can provide an estimate of the parameter. f always falls between 0 and 1 because it describes the fraction of theoretical flux that is truly occurring in the system. These equations can be applied to packed column and other reactor geometries by adding more reactors in series.

2.5 Model Evaluation

Analysis of a model and the fit to experimental data can be conducted using statistical analysis. Linear sum of squares of the residual error (SSE) is an accurate and common method for measuring the variation and deviation from theory. This basic analysis method is shown in *Equation 10* below.

$$SSE = \Sigma(y - \hat{y})^2 \tag{10}$$

In the equation, the difference between the model simulated values and the experimental values are squared and summed to get an idea of the level of fit for the model. The lower the value, the better the fit of the model.

CHAPTER 3
MATERIALS AND METHODS

SECTION 1

3.1 Methanotrophic activity analysis in batch and continuous flow reactors

3.1.1. Culture growth (OB3b and 5GB1)

OB3b was obtained from Dr. Lisa Stein from University of Edmonton. OB3b was grown in a low salt media with nitrate mineral salts (NMS) buffered with carbonate and phosphate to a pH of around 7.5 (in the appendix). Stock cultures were used for 10% cultures inoculations, and were grown while shaking at 300 rpm and 30°C in 500 mL bottles with 150 mL of media and a 20% methane headspace in air (methane obtained from Industrial Welding in Albany, OR). Cultures were grown until desired protein densities were measured using optical density (normally 3 to 4 days). 500 mL Wheaton media bottles with caps containing Wheaton 20 mm gray butyl septa were used for growth. All culture transfers were prepared in a laminar flow hood and bottles were autoclaved before and after use to maintain aseptic conditions.

5GB1 was obtained from Dr. Mary Lidstrom at the University of Washington. It was grown similarly to OB3b, but with a higher salt content media with a pH of 9.5. The media recipe was provided by the University of Washington (in the appendix). 5GB1 was also grown at 300 rpm and 30°C in 500 mL bottles with 150 mL of media and a 20% methane headspace in air, until desired protein densities were attained.

3.1.2. Culture harvesting

After cultures were grown in batch to desired protein densities, they were collected and centrifuged at 9000 rpm for 15 minutes using 50 mL Falcon centrifuge tubes. A resulting culture pellet is shown in *Figure 6.* The pelleted cultures were resuspended in fresh media depending on the experimental requirements. An aliquot of the dense culture mixture was used for microburet protein assay for total protein measurements (Gornall et al., 1949). The solution was then either left in suspension or was immobilized in alginate or agarose. Sodium alginate (Alginic acid, sodium salt; Algin) from Spectrum Chemical MFG. Corp. in Gardena, CA and low melt agarose from IBI Scientific in Kapp Court Peosta, IA.

Figure 6. Pelleted OB3b culture after being centrifuged for 15 minutes at 9000 rpm.

3.1.3. Immobilization methods

3.1.3. i. Alginate immobilization

A stock solution of 4 wt% alginate was prepared through small additions of powdered alginate to constantly mixed water. The final solution was autoclaved to ensure no contaminations were present. Pelleted methanotroph bacteria was re-suspended in media and mixed with 4 wt% sodium alginate solution to make a final 2 wt% alginate solution containing the culture. The alginate and cell mixture was dropped from a syringe and 23G needle, using a Thermo Scientific Orion M361 Sage Syringe Pump, into a solution of 0.1 molar $CaCl_2$ solution for external cross-linking to occur (*Figure 7*). Beads were rinsed with deionized water 3 times to ensure minimum calcium remained in the surrounding media. Beads were then either

resuspended in media or packed into an up-flow column. Average bead size was 2.9 ±

0.0 mm.
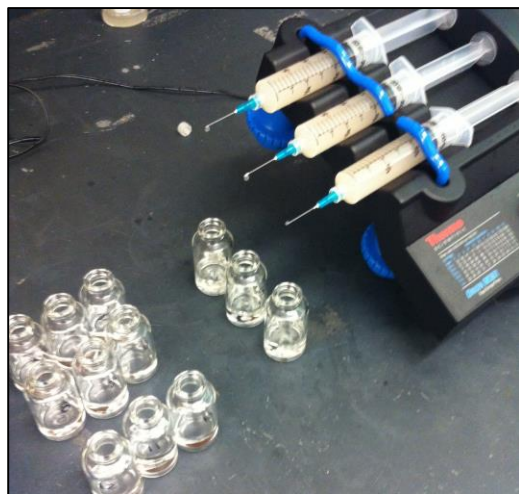
Figure 7. Alginate solution in a syringe dropped into vials containing CaCl$_2$ solution for external cross-linking.

3.1.3. ii. Agarose immobilization

Agarose powder was added to DI water to make a 2 wt% solution and heated

to 60°F. The heated agarose was allowed to cool to 30°F and the dense methanotroph

bacteria in media solution was mixed into the gel. Beads were individually formed,

by extruding the agarose solution through a 23G needle using a syringe pump. The

beads were dropped onto a Parafilm and allowed to cool, forming stable beads. The

beads have a flat bottom and a spherical top, forming a hemi-sphere. These beads had

an average diameter of 3.1 ± 0.6 mm and are shown in *Figure 8*.

Figure 8. Agarose beads cooling after dropping onto the wax paper using the syringe pump.

3.1.4. Batch testing

Batch tests for both cultures were conducted using 70 mL glass vials with either suspended or immobilized cultures. Testing for both cultures and immobilization methods follow the same procedure from this point on. For suspension batch testing, 5 mL of culture suspension were added to the 70 mL vials. For immobilized culture testing, 5 mL of hydrogel beads with 4 mL of fresh media were added to each vial. Methane was added (at volumes ranging from 1-3 mL) to the headspace consisting of air. *Figure 9* shows examples of beads in the batch vials. Vials were shaken at 20°C and 300 rpm using a shaker table to ensure equilibrium was reached between the liquid and gas phase. 100 μL headspace samples were injected on the gas chromatograph (described in later section) using a Hamilton Co. Microliter Gastight Syringe to measure methane consumption over varying lengths of time.

Figure 9. OB3b immobilized in alginate beads in batch reactor vials. All vials contain hydrogel beads, media, and a headspace of air with methane additions.

3.1.4. i Kinetic parameter verification experiments

Experiments were conducted to compare activities of suspended cultures to their immobilized forms. Equivalent protein concentrations in batch reactors were compared for each immobilization method studied. Protein concentrations between 0.42 and 1.62 mg protein/mL of bead were used for both OB3b in alginate beads and 5GB1 in agarose beads. Three mL of methane were added to headspace and consumption was monitored using headspace injections on the GC until the methane was fully consumed.

3.1.5. Gas chromatograph sample testing methods

Gas chromatography was used to determine methane concentration of both headspace and liquid samples. Samples of 2 µL liquid or 100 µL headspace (depending on experiment requirements) were injected into a column with 200°C injection port and 50°C column temperature. Headspace methane concentrations were measured by injecting a 100 µL sample onto a Shimadzu Corporation gas chromatograph Model GC-8A using nitrogen as the carrier gas using a flame-ionized detector. Chromatographic separation was achieved using a Supelco (Bellefonte, PA) 80/100 Carbopack™ C/0.2% Carbowax 1500 column. Triplicates of each sample

were run to guarantee validity of the results. The headspace concentration was used

with Henry's Law Constant for methane (H_{cc} = 31.25) to determine concentration in

the liquid phase, and to create a total mass balance. The same procedure was followed

for liquid injections of 2 µL volume. The concentrations were determined using

external standards to make calibration curves and were used for concentration

estimates (example in the appendix). Column operation was maintained at these

conditions for the duration of all experiments. A new column was implemented half

way through experimentation, but calibration tests were conducted to ensure that the

data was comparable.

For methanol production, experiments a stock solution of methanol was used

to create standards measured using the liquid injection method on the GC. Retention

times and concentrations from these calibration tests were used for comparison for

methanol accumulation experiments in batch and column testing.

3.1.6. Packed column

3.1.6. i. Packed column setup

The packed column experiments were conducted with small glass column

with a 2.5 cm inner diameter and a height of 7 cm. Metal filter screens on the influent

and effluent supported the bead pack. Tubing connected the influent media bottles to

the packed column and sample ports were created using a three–way valve connector.

The column was packed wet with beads containing the immobilized cultures and

plumbing was attached to create an up flow setting. Media was added to the column

until all pore volume was the liquid phase. Column setup shown in *Figure 10* and a

flow diagram of the setup shown in *Figure 11.* The total volume of beads packed was

consistently around 30 mL with an average pore volume between 5 and 10 mL. Pore volumes were measured by weighing the column before and after filling the void space. Two 3 mL plastic syringes were used at each sample port to extract samples of 1 mL volume from the influent and effluent. A 2 μL sample was taken from these syringes and injected onto the GC immediately after collection.
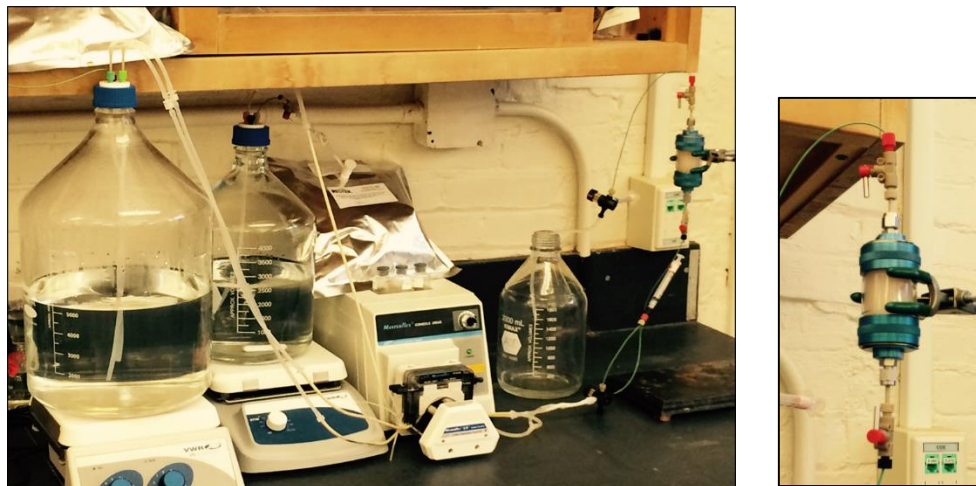
Figure 10. Packed column setup (left) including media bottles with methane and oxygen headspace, tubing to column, peristaltic pump, samples ports and packed column. Close up of packed column (right).

Saturated solutions with either methane or oxygen were prepared in two large reservoirs and were fed to the column. To ensure the media was fully saturated both the methane and oxygen reservoirs were stirred using VWR Hotplate/Stirrer stir plates with magnetic stir bars for 30 minutes before solution passed through the column. The bottles were originally filled completely with media and gas was allowed to flow into the bottles while forcing the media out, creating a headspace of only methane (or oxygen). Media saturated with methane or oxygen was flowed up through the column at two parts oxygen and one part methane at flow rates ranging from 1-10 mL/min using a Cole Parmer Masterflex L/S model 7519-06 Cartridge Pump. Flow rate settings were calibrated by passing the media through the column at

increasing setting and measuring the effluent volumetric flow rate. Pump calibrations were conducted before starting each experiment to verify packed methods remained consistent. Examples of the liquid flow rate calibrations are in the appendix.
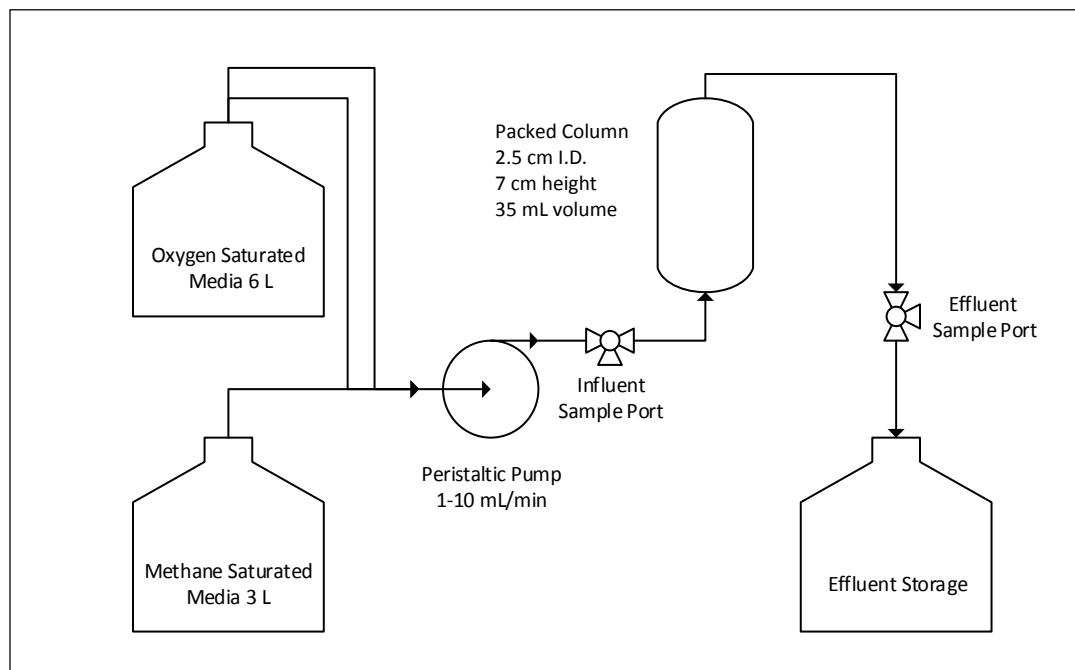
Figure 11. Schematic of the packed column setup. Media is pumped from storage reservoirs through the packed column and into the effluent bottle. Sample ports consisted of a 3-way valve connectors with 3 mL syringes attached for liquid sample extraction.

3.1.6. ii. Packed column operational methods

The column was packed with gel beads that had an average size of 3 mm in diameter. The cell concentrations were varied in the beads so that the protein ranged from 0.9- 18 mg protein/mL bead. Fluid pump rates were varied to achieve residence times ranging from 1-10 minutes, depending on experimental conditions. The column was run for 30-60 minutes before samples were taken to ensure steady state had been reached. Triplicate samples were drawn from the column for each residence time tested allowing 30-60 minutes between each measurement to ensure steady state was achieved. An example of a typical result from one column experiment is shown

Figure 12. 5GB1 was immobilized in agarose beads at a protein concentration of 1.8

mg protein/mL beads. Influent and effluent concentrations were measured for both

OB3b and 5GB1 for different protein concentrations and different residence times to

calculate fraction of methane consumed. As shown in *Figure 12*, very reproducible

estimates of the extent of methane utilization were obtained.
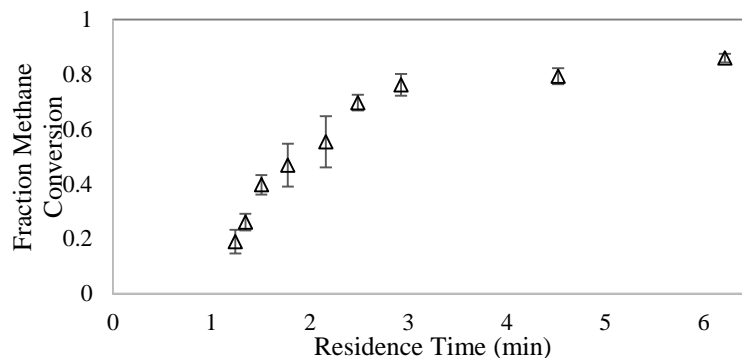
Figure 12. Example result from packed column experiment. 5GB1 was immobilized in agarose beads and methane consumption measured at increasing residence times. Error bars represent variation in triplicate measurements.

OB3b bacteria was immobilized in agarose and alginate at similar protein

concentrations to ensure that the activity measurements were comparable for both

methods of immobilization. For this experiment, OB3b was immobilized in agarose

hydrogels via the same procedure used for the 5GB1, with the exception of the media

used.

3.1.7. Methods of analysis

3.1.7. i Batch kinetic analysis

Two important parameters for each culture are the max substrate utilization

rate (K_{max}) and the half saturation coefficient (K_s) associated with the Monod kinetics.

The Michaelis-Menten and Monod equations are often used when evaluating batch

kinetic tests. Substrate reaction rate for a bacterial culture is shown in *Equation 11*.

$$-\frac{dC_L}{dt} = \frac{K_{max}X_aC_L}{(K_S+C_L)} \tag{11}$$

This equation can be integrated and manipulated to fit substrate consumption data for changing protein concentrations. A common method of integration and application is applied for solve for unknown kinetic parameters (Smith & McCarty, 1997). *Equation 12* represents the growth of bacteria within the system for changing substrate concentrations. This version of the Monod equation does not include cell decay. The next equation, *Equation 13,* is the analytical solution. This method is shown in the following equations:

$$X_a = X_{a,0} + Y(C_{L,0} - C_L) \tag{12}$$

$$t = \frac{1}{K_{max,app}} \left\{ \begin{array}{l} \frac{k_s}{X_{a0}+YC_{L0}}\ln(X_{a0} + Y(C_{L0} - C_L)) + \frac{k_s}{X_{a0}+YC_{L0}}\ln\left(\frac{C_{L0}}{X_{a0}C_L}\right) \dots \\ \dots + \frac{1}{Y}\ln(X_{a0} + Y(C_{L0} - YC_L)) - \frac{1}{Y}\ln(X_{a0}) \end{array} \right\} \tag{13a}$$

With *t* being time, $K_{max,app}$ as the apparent maximum substrate utilization rate, K_s as the half saturation coefficient, $X_{a0,}$ as the initial biomass protein concentration, Y as the cell yield coefficient, and C_L the substrate concentration in the liquid phase.

Batch kinetic tests can be conducted for substrate consumption for any given parameters (protein concentrations, substrate concentrations, and free or immobilized cultures). The model is then used in conjunction with the substrate consumption data and is fit to find kinetic parameter estimates ($K_{max,app}$ *and* K_s) for a given culture. For short term test with high biomass concentration the biomass remain constant at X_{a0}.

Two phase batch testing (liquid and headspace) require a second step in the kinetic analysis. The model and parameters are dependent on only the liquid substrate concentration, with no consideration of the substrate in the headspace. The $K_{max,app}$

determined through the analysis is not the true maximum substrate utilization rate.

Incorporation of Henry's law constant is required to convert the pseudo rate to the

actual, shown in *Equation 13b*.

$$K_{max,app} = \frac{K_{max,true} * V_L}{V_L + V_G H_{cc}}$$ (13b)

With V_L as the volume of liquid in the batch reactor, V_G as the volume of gas

in the batch reactor, and H_{cc} as the dimensionless Henry's law coefficient.

Experimental values are applied to calculate the true substrate utilization rate within

the batch reactors.

3.1.7. ii. CMBR modeling – packed column comparison

Modeling of a packed column system can be done effectively using a

completely mixed biofilm reactors (CMBRs) in series. Mass balances, diffusion

equations, and rate kinetics can be applied to a CMBR configuration to simulate

reactor behavior. A fully developed model commonly used is one derived from Fick's

Law for diffusion and Monod kinetics for substrate utilization (Rittmann & McCarty,

2001) (Usha et al., 2012). The main assumptions for model derivation are represented

by the following boundary conditions:

- Substrate concentrations at the biofilm and media interface are equal; the

  boundary condition at the liquid-film interface is shown in *Equation 14*, with *J* as

  the flux, *D* as the diffusion coefficient, *S* as the substrate concentration, and *z* as

  the biofilm thickness.

$$J = \frac{D}{L}(S - S_s) = D_f \left.\frac{dS_f}{dz}\right|_{z=0} = D \left.\frac{dS}{dz}\right|_{z=0}$$ (14)

- Substrate flux at surface of film attachment is zero, *Equation 15*, with L_f as the

  depth into the biofilm.

$$\frac{dS_f}{dz}\bigg|_{z=L_f} = 0 \tag{15}$$

Figure 13 represents CMBRs in series and the relevant parameters. Media

flows into the first reactor, diffuses into the biofilm where it is transformed, and the

substrate that is not utilized flows out of the reactor in the effluent stream to the next

reactor. Therefore $S_{eff,1}$ equals $S_{inf,2,}$ and the process continues.
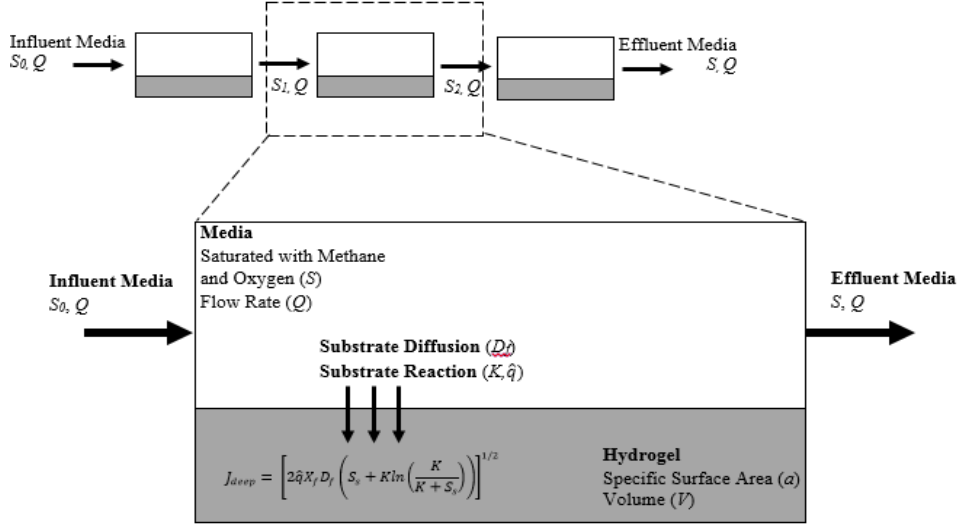
Figure 13. Schematic describing the 3 CMBR model. Influent media contain substrate diffuses into the biofilm where is reacts based on system kinetics. The effluent of that reactor then flows into the next reactor in series.

Parameters of importance for the system are the substrate concentration (S),

protein concentration (X_f) media flow rate (Q), biofilm thickness (z), biofilm specific

surface area (a), diffusion into the biofilm (D), substrate utilization rates, and total

reactor volume (V). Substrate utilization and diffusion into the biofilm at steady state

are described in *Equation 16*. The first term represents substrate diffusion into the

biofilm in the z-direction and the second represents substrate utilization by the active

culture.

$$0 = D_f \frac{d^2 S_f}{dz^2} - \frac{K_{max}X_f S_f}{K_S + S_f} \tag{16}$$

Equation 17 is the general analytical solution for *Equation 16* applying

previously explained boundary conditions. Concentrations at both boundaries biofilm

(interfacial and bottom) must be known or assumed for this equation to be valid.

$$J_{deep} = \left[2K_{max}X_f D_f \left(S_s + K_s ln \left(\frac{K_s}{K_s + S_s} \right) \right) \right]^{1/2} \tag{17}$$

The steady state mass balance on a substrate in a CMBR is shown in *Equation*

18 (Rittmann & McCarty, 2001). This balance is specifically derived for a biofilm

within a CMBR with the substrate diffusing into the film. The flux term incorporates

both the substrate utilization and diffusion.

$$0 = Q(S^0 - S) - J_{ss}aV \tag{18}$$

S is the substrate concentration exiting the reactor, S_0 is initial substrate

concentration into the reactor, *a* is the specific film surface area in reactor, *V* is the

volume in the reactor, *Q* is the flow rate of fluid through the column, and J_{ss} is the

steady state substrate flux into the biofilm. Assuming that the film is deep, the general

solution to the flux equation can be combined with the reactor mass balance. The

final combined equation is shown in *Equation 19.*

$$0 = Q(S_s - S) - aV * \left[2K_{max}X_f D_f \left(S_s + K_s ln \left(\frac{K_s}{K + S_s} \right) \right) \right]^{1/2} \tag{19}$$

Experimental parameters are input into the equation and the only unknown

(the final effluent substrate concentration) can be solved. This value can be compared

to experimental results to better understand the behavior of a reactor. The setup of the

model is further presented in the appendix.

SECTION 2

3.2 External and internal gelation for OB3b in alginate beads

3.2.1. Internal gelation Method #1

All internal gelation testing was conducted using OB3b culture, grown in the same method described previously. The internal gelation procedure is as follows: A 1 M solution of glucono-δ-lactone (GDL) and a 1 M solution of $CaCO_3$ are prepared. 4 wt% alginate solution and cell suspension are placed in separate vials. 400 μL $CaCO_3$ are added to 10 mL alginate and 800 μL GDL added to 10 mL of cell suspension. The solutions are combined and stirred for 30 seconds. The solution is dropped into media using syringe, 23G needle, and syringe pump. 70 mL vials with gray butyl septum and a crimp top were used for batch testing.

3.2.2. Internal gelation Method #2

A second method of internal gelation was also investigated. The exposure to the pH of the $CaCO_3$ solution was observed to be harmful to the culture, so the procedure was modified. The new method requires the cell suspension to be added to the GDL and $CaCO_3$ combined solution. This ensures that the pH is near neutral and safe for cell exposure. The procedure is as follows: A 1 M solution of glucono-δ-lactone (GDL) and 1 M solution of $CaCO_3$ were prepared. 4 wt% alginate and media are placed in separate vials. 400 μL $CaCO_3$ was added to 10 mL alginate and 800 μL GDL to the 10 mL of media. Both solutions were combined and cell suspension was added. Solution was stirred for 30 seconds and dropped into media. 70 mL vials with gray butyl septum and a crimp top were used for testing. Beads were then used for batch activity testing.

3.2.3. Ethylene to ethylene oxide activity testing

OB3b has the ability to utilize ethylene and convert it to ethylene oxide (ETO) using the MMO enzyme. This test method is commonly used for cell activity assays because measureable levels of ETO are produced rapidly (Mehta, Mishra, Ghose, 1991). Ethylene was added to the headspace of each vial, in volumes ranging from 1-3 mL. Protein concentrations ranged from 0.5-1.0 mg protein/mL bead. The production of ETO was measured using headspace analysis on the GC using the same method as described in the earlier. Activity comparisons of suspended, internal gelation, and external gelation were conducted for OB3b.

SECTION 3

3.3 Production of methanol through inhibition of the OB3b MDH enzyme

3.3.1. Inhibition of MDH with cyclopropane

Production of methanol by OB3b required the chemical inhibition of the MDH enzyme using cyclopropane or cyclopropanol (Shimoda & Okura, 1990). When cyclopropane is introduced to the culture, it is converted to cyclopropanol which inhibits MDH. Evaluate of inhibition effectiveness included both cyclopropane and cyclopropanol as inhibitors. OB3b was immobilized in alginate for these tests Cultures were then exposed to cyclopropane from Matheson Gas Company (Newark, NJ) by adding 100 µM to the reactor headspace. Headspace samples were measured using the GC to monitor the consumption of cyclopropane, with a retention time of 1.1 min, using same procedure as previously described. After 2, 6, or 18 hour exposure, vials were opened and beads were rinsed using DI water three times to

ensure no cyclopropane was remaining. Methane was added to the vials and methane

consumption and methanol production were monitored using headspace injections on

the GC over time. After methanol production ceased, media was again rinsed three

times with DI water and the methanol production process was repeated.

3.3.2. Cyclopropanol inhibition

When OB3b is exposed to cyclopropane, it is converted to cyclopropanol.

The produced cyclopropanol can be used as an MDH inhibitor. A stock solution of

purchased cyclopropanol from Manchester Organics (Cheshire, U.K) was compared

to the experimentally produced solution to ensure that they were the same compound.

After the determination of concentrations of the stock solutions, the biologically

generated cyclopropanol was used for inhibition testing. The column was packed with

immobilized OB3b beads and a diluted cyclopropanol solution was passed through

the column using a syringe pump. Cyclopropanol concentrations ranging from 0.05-

0.25 mM were introduced to the column. After exposure, the flow was stopped and

the culture was exposed to the cyclopropanol for 18 hours. Fresh media was then

flushed the column until no cyclopropanol remained. A mixture of methane and

oxygen saturated media was then passed through the column. Methane consumption

and methanol production were measured using liquid injections on the GC. After

methanol production ceased, the column was re-inhibited using the procedure

previously described and the methanol production phase was repeated.

3.4 Summary table of relevant experiments

The following table describes relevant experiments conducted, the culture used, the initial substrate concentration, the protein concentrations, immobilization method, and methane utilization rates.

Table 1. List of all relevant experiments in both batch and column research.

	Culture Type	Protein Concentration (mg protein/mL)	Immobilization Type	Normalized Methane Consumption Rate (mg CH$_4$/mg protein/min)	Experiment Description
				Batch Experiments	
#1	OB3b	0.52, 1.62	Alginate	0.0089	Monod experiment, full consumption of methane
#2	OB3b	0.3	Suspension	0.0110	Experiment displaying highest methane utilization
#3	OB3b	7.9	Alginate	0.0012	Experiment displaying lowest methane utilization
#4	OB3b	0.16-11	Suspension and Alginate	0.0019	Ranges for all OB3b experiments and average methane utilization rate
#5	OB3b	0.5	Alginate	0.0013	Sequencing batch reactor for methanol production experiment (inhibition)
#6	5GB1	0.42, 1.62	Agarose	0.0093	Monod experiment, full consumption of methane
#7	5GB1	0.4	Suspension	0.0111	Experiment displaying highest methane utilization
#8	5GB1	15	Agarose	0.0009	Experiment displaying lowest methane utilization
#9	5GB1	0.4-15	Suspension and Agarose	0.0025	Ranges for all 5GB1 experiments and average methane utilization rate
				Column Experiments	
#10	OB3b	3.1-18	Alginate	0.001-0.012	Packed column, ranges for all OB3b column experiments
#11	OB3b	3.3	Agarose	0.001-0.012	Packed column immobilization method comparison experiment
#12	OB3b	10	Alginate	0.001-0.012	Packed column methanol production
#13	5GB1	0.9-6.5	Agarose	0.001-0.012	Packed column, ranges for all 5GB1 column experiments

CHAPTER 4
RESULTS

SECTION 1

4.1 Methanotrophic activity analysis

Activity differences between the two methanotrophs, OB3b and 5GB1, were

measured for suspended and immobilized cultures. Batch kinetic testing was

conducted to monitor the consumption of methane for activity determination. Small

vials were prepared with free or immobilized cultures to investigate these phenomena.

4.1.1. Kinetic batch testing results

Batch reactor vials containing immobilized cultures at protein concentrations

ranging from 0.42-1.62 mg protein/mL bead were directly compared to free cultures

in experiments allowing complete consumption of methane. Methane was added to

the headspace of each vial and measurements were taken until methane was

completely consumed. Results from these experiments are shown in *Figure 14a* for

the suspended cultures and *Figure 14b* for the immobilized cultures. Each time point

represents an average of triplicate vials with the same protein concentration. The

figure shows the high and low protein concentrations of suspended cultures, for both

5GB1 and OB3b. Error bars represent standard deviation of the triplicate

measurements. A high and low protein concentration were tested for 5GB1 in agarose

and OB3b in alginate to determine if the fitted parameters were valid at multiple

protein concentrations. Results were fit using the integrated Monod curve to solve for

the kinetic parameters maximum specific substrate utilization, $K_{max,}$ and the half

saturation coefficient, K_s. All parameters used in the model are listed in the appendix.

An excellent match of the model to the experimental data is shown.
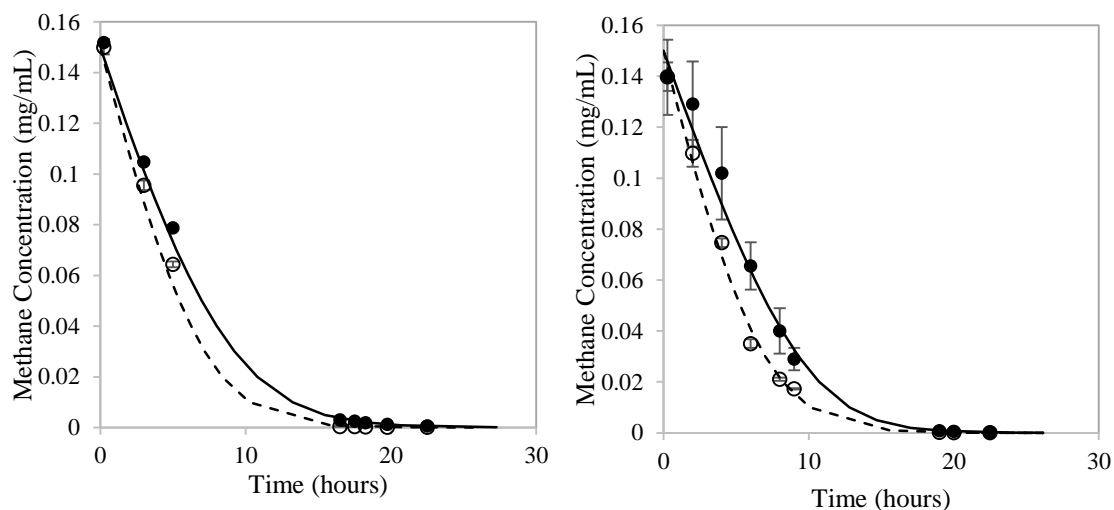
Figue 14a. Methane consumption curves for suspended 5GB1 (left) and OB3b (right) for integrated Monod evaluation. 5GB1 has protein concentrations of 1.46 (○) and 0.42 (●) mg protein/mL. OB3b has concentrations of 1.62 (○) and 0.52 (●) mg protein/mL.

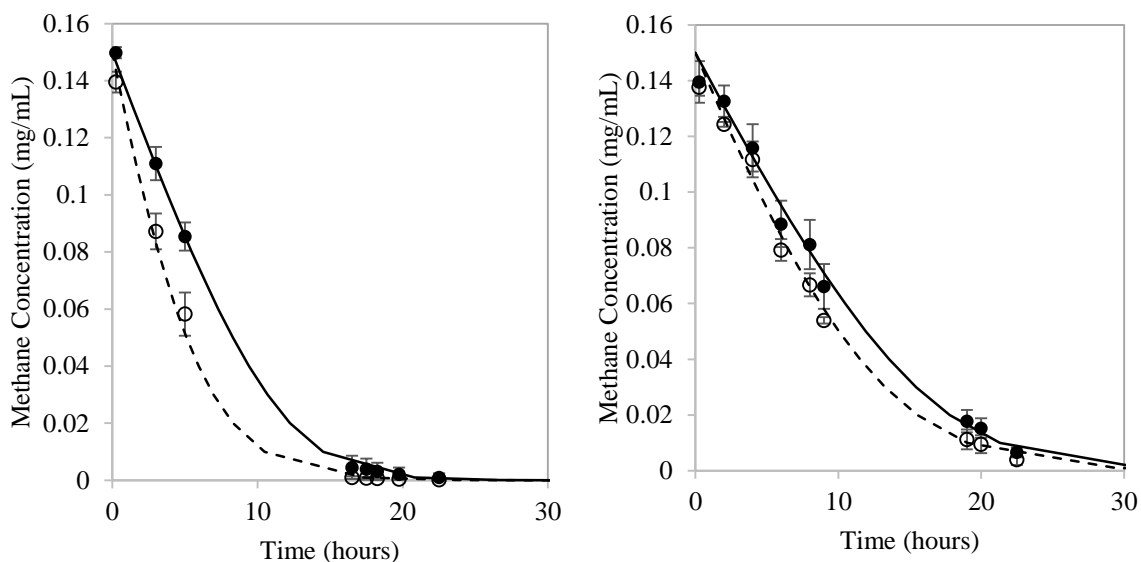**Figue 14b.** Methane consumption curves for immobilized 5GB1 (left) and OB3b (right) for integrated Monod evaluation. 5GB1 has protein concentrations of 1.46 (○) and 0.42 (●) mg protein/mL bead. OB3b has concentrations of 1.62 (○) and 0.52 (●) mg protein/mL bead.

Kinetic parameters listed in *Table 2* were determined with the integrated

Monod equation, the pseudo K_{max}, and the experimental results. Initial substrate

concentration, active protein concentration, and the cell yield coefficient were all held constant while the kinetic parameters K_s and K_{max} were varied using Excel Solver to achieve a best fit. Two protein concentrations were tested for each culture type, and parameters were altered to fit both simultaneously.

Table 2. Experimentally determined kinetic parameters for OB3b and 5GB1 in immobilized and suspended forms. Standard deviations are based on triplicate measurements. Lower case letters indicate statistical significant differences for kinetic parameters.

Culture Type	K_s (mg CH$_4$/L)	K_{max} (mg CH$_4$/mg protein/min)
OB3b Suspended	2.3 ± 0.3 [a]	0.0089 ± 0.0009 [c]
OB3b Immobilized	3.4 ± 0.3 [b]	0.0085 ± 0.001 [c]
5GB1 Suspended	1.9 ± 0.2 [a]	0.0093 ± 0.004 [c]
5GB1 Immobilized	3.1 ± 0.4 [b]	0.0088 ± 0.001 [c]
Lee et al., 2006 OB3b Suspension	1.47	0.011

Evaluations were conducted to determine whether the parameters were significantly different for suspended and immobilized cultures. Final model parameters were lower, but comparable to previously reported values obtained in suspended cultures for OB3b shown in *Table 2* (Lee et al., 2006). There are currently few published parameters for 5GB1, however experimental results indicate a higher rate than OB3b but the increase is not significant. A statistical analysis indicated that the K_s values are statistically different for the immobilized and suspended cultures. The raised K_s for the immobilized cultures are representative of the slight transport limitations seen in the substrate diffusion. A common method for representation of an immobilized system is to increase the K_s as described in Stewart, 2003.

4.1.2. Packed column results

4.1.2. i. Immobilization method comparison

Alginate and agarose immobilization methods were evaluated for their effects on culture activity. Comparisons will confirm higher experimental rates of 5GB1 are independent of any diffusion differences in agarose vs. alginate. An experiment was conducted using OB3b in both agarose and alginate gel beads. Agarose beads with an OB3b protein concentration of 3.3 mg protein/mL bead were made and packed into the column. This protein concentration was selected because it falls near a previously conducted packed column experiment with OB3b in alginate gel beads at 3.1 mg protein/mL bead. Methane consumption was measured for residence times from 1-6 minutes at each protein concentration (*Figure 15*).
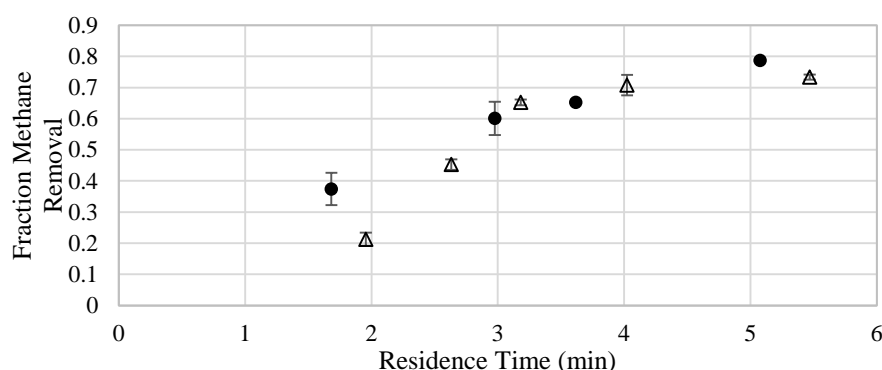
Figure 15. OB3b immobilized in alginate at 3.3 mg protein/mL bead (Δ) and agarose at 3.1 mg protein/mL bead (●) at increasing residence times. Both methods of immobilization are shown for a comparison of methane consumption. Residence times were increased to evaluate performance.

Methane consumption was measured at increasing residence times for agarose and alginate immobilized OB3b. The culture retained a similar level of activity when immobilized in agarose or alginate gels beads. Therefore, immobilization method does not contribute a significant difference in methane consumption activity. Results indicate the higher rates of immobilized 5GB1 that will be presented, are attributed to the activity of the culture, and not to changes in immobilization method. The column test demonstrated that alginate and agarose achieved the same methane consumption.

Agarose and alginate have been reported to have different effects on substrate diffusion, however, they are of a similar magnitude (Li et al., 1996). With the results of this experiment, and for simplification purposes, both alginate and agarose diffusion will be represented using the same diffusion coefficient in all modeling applications.

4.1.2. ii. Packed column activity testing

For determination of optimal parameter settings in the packed column, culture type, residence time, and protein concentration were varied. For the different experiments the column was packed with the protein concentrations 3.1, 6.0, 9.3, and 18 mg protein/mL bead with OB3b and 0.9, 1.8, 3.2, and 6.6 mg protein/mL bead with 5GB1 (in alginate and agarose gel beads, respectively). Saturated methane and oxygen solutions combined at a 1:2 ratio were passed through the column at increasing residence times. One mL influent and effluent samples were taken at each residence time and measured using 2 μL liquid injections on the GC to calculate the levels of methane consumption. In order to achieve steady state, the column was run for 30-60 minutes at each residence time before triplicate samples were taken. Results from all experiments are shown in *Figure 16.* Each point on the figure represents the average methane consumption measured from samples taken at the given residence time and error bars represent the standard deviation.
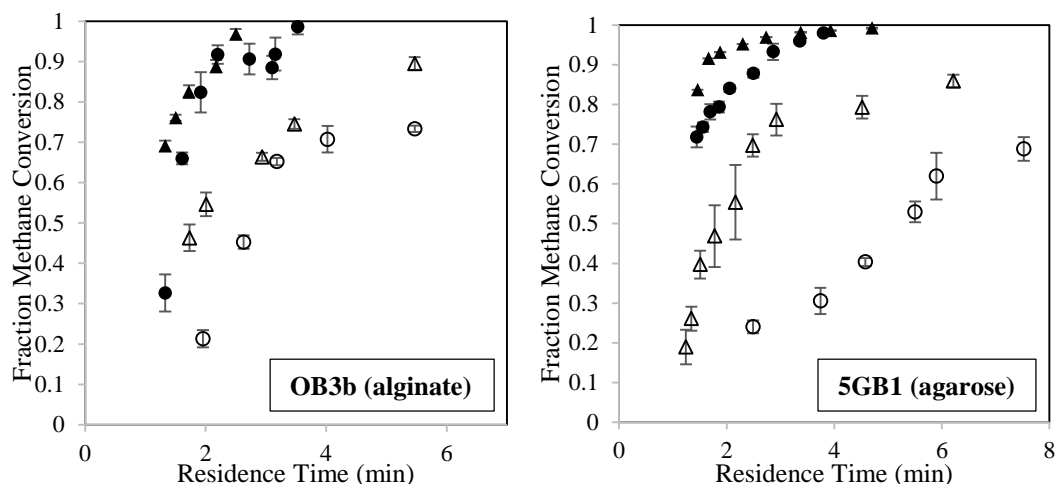
Figure 16. Results of continuous flow packed column studies. Methane utilization is plotted as a function of hydraulic residence time. OB3b immobilized in alginate (left) at 3.1 (○), 6.0 (Δ), 9.3(●), and 18 (▲) mg protein/mL bead. Error bars show standard deviation of triplicate measurements. 5GB1 immobilized in agarose (right) at 0.9 (○), 1.8 (Δ), 3.2(●), and 6.6 (▲) mg protein/mL bead. Error bars show standard deviation of triplicate measurements.

General trends seen in the methane consumption behavior are as follows: an increase in protein concentration led to decreased residence time required for removal and as residence time, at a constant protein concentration, increased the total methane conversion increased. These phenomena were seen in both OB3b and 5GB1 tests. Comparison of the 5GB1 and OB3b experiments indicated that the 5GB1 performed at a higher rate, consistent with batch experiments. 5GB1 is as capable of converting equal concentrations of methane as OB3b, but at a much lower protein concentration. For example, a protein concentration of 3.1 mg protein/mL bead OB3b removes 50% of the methane at a residence time of 3 minutes, whereas a protein concentration of 3.2 mg protein/mL bead of 5GB1 can accomplish nearly 95% removal at the 3 minute residence time. 5GB1 exhibited a higher rate of methane consumption activity than OB3b in both batch and packed column reactors. However, some of the other differences contributing to the increased performance are the specific surface area, the total number of beads in the system, and the column void space.

For verification that the experimental trends follow theory, the model developed by Rittmann and McCarty for biofilm diffusion was applied to experimental data. 3 CMBRs in series were modeled using the methods previously described. *Table 3* provides model input parameters (an expanded version of this table is shown in the appendix for specific inputs for respective cultures).

Table 3. List of parameters, values, units, and descriptions for the 3 CMBR model. Ranges indicate experimental variability and variations between OB3b and 5GB1. Discussion of parameter determination in the appendix.

Parameter	Value Range	Units	Description
X_f	0.5 - 20	(mg protein/mL bead)	Concentration of active protein
a	10-20	(cm^2/cm^3)	Specific surface area
S_0	7.2-7.9	(mg CH_4/mL)	Inlet liquid phase substrate concentration
K_{max}	0.0089-0.0093	(mg CH_4/mg protein/min)	Maximum specific rate of substrate utilization
D_f	0.001	(cm^2/min)	Diffusion coefficient
S_s	7.2-7.9	(mg CH_4/mL)	Liquid phase substrate concentration
K_s	1.9-2.3	(mg CH_4/L)	Half-saturation coefficient

Specific surface area, inlet substrate concentration, maximum substrate utilization rate, diffusion coefficient, and the half saturation coefficient were held constant through each experiment. Protein concentration was the only changing parameter in the experiments and model inputs aligned with this as well. All parameters were selected based on experimental settings, so variations between experiments were seen for inlet methane and total bead volume (influencing *a*).

Protein concentration was changed to represent the conditions as measured in experimentation.

The K_{max} and K_s applied to the model are the parameters determined in batch for suspended OB3b and 5GB1. The CMBR model takes substrate diffusion into account, so suspended parameters meet model requirements more accurately.

Final model parameters were applied to the packed column experimental data (from *Figure 16*) and are shown in *Figures 17* and *18*. Without fitting any parameters, the model accurately followed basic trends in experimental data. Increases in methane consumption with respect to increasing protein concentration are well described by the model. Also, the diminishing return of increasing protein is represented by the model, meaning large increases in protein concentration do not provide equally large increases in methane consumption.
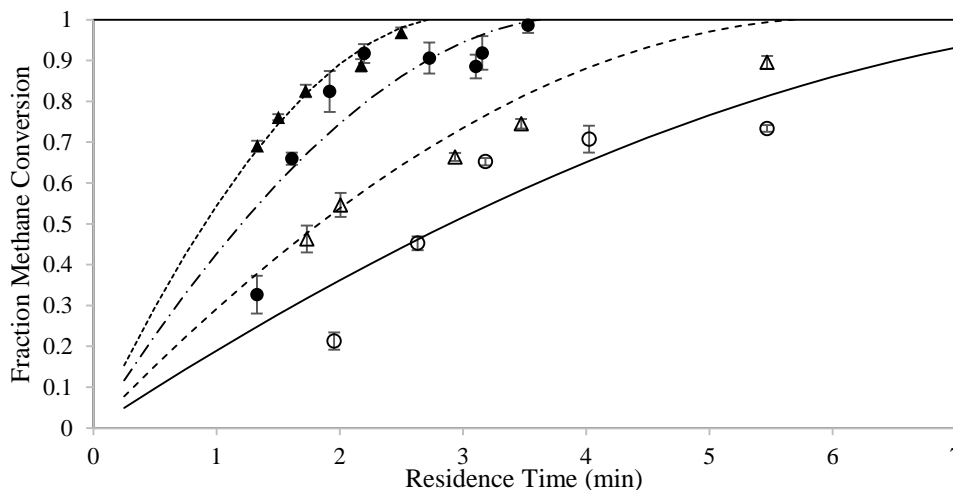
Figure 17. OB3b immobilized in alginate at 3.1 (○), 6.0 (Δ), 9.3(●), and 18 (▲) mg protein/mL bead. Error bars show standard deviation of triplicate measurements. Lines represent the 3 CMBR model for each corresponding protein concentration.
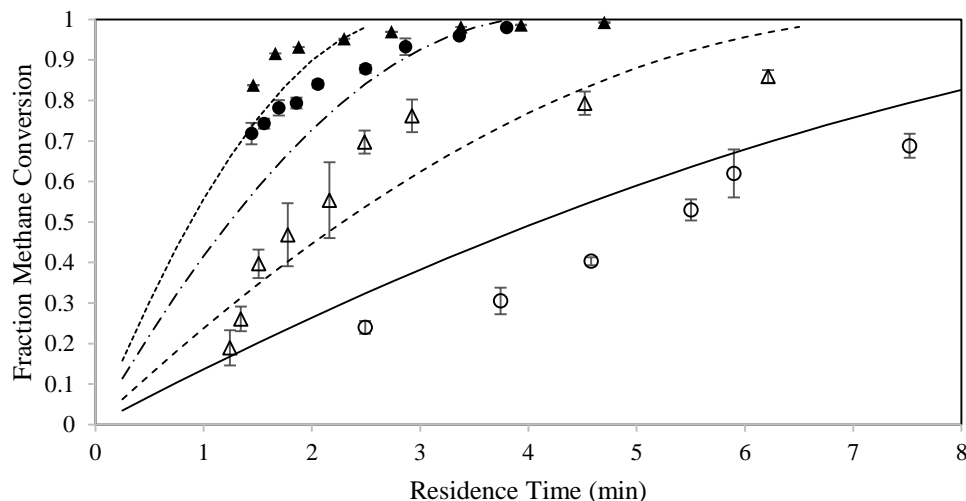
Figure 18. 5GB1 immobilized in agarose at 0.9 (○), 1.8 (△), 3.2(●), and 6.6 (▲) mg protein/mL bead. Error bars show standard deviation of triplicate measurements. Lines represent the 3 CMBR model for each corresponding protein concentration.

Analysis of the model fit to experimental values was conducted using the sum of squared errors analysis method. The model fits the data with a SSE value for all protein concentrations combined of 0.143 and 0.372 for OB3b and 5GB1, respectively. While not perfect, the fit simulates well the effects of increasing protein on methane consumption and the change the residence time has on the extent of consumption achieved.

4.1.2.iii. Parameter sensitivity analysis – 5GB1 only

A sensitivity analysis for the 5GB1 tests was conducted on three important CMBR parameters, the half saturation coefficient K_s, diffusion coefficient D_f, and the substrate influent concentration S_s. The standard parameters are shown in the appendix for the base case model comparison. A standard protein concentration of 5 mg protein/ mL bead was selected for the analysis. The base standard K_s value of 1.9 mg CH_4/mL (measured in suspended batch experiments) was compared to a doubled value (3.8 mg CH_4/mL) and a halved value (0.95 mg CH_4/mL). *Figure 19* shows the

results of the sensitivity analysis. An increase in K_s led to a slight decrease in fraction of methane conversion. The effects of variation of this parameter are small, but some shift in estimated consumption is shown. A decrease in the K_s indicates a lower residence time required to achieve a specific extent of methane consumption.
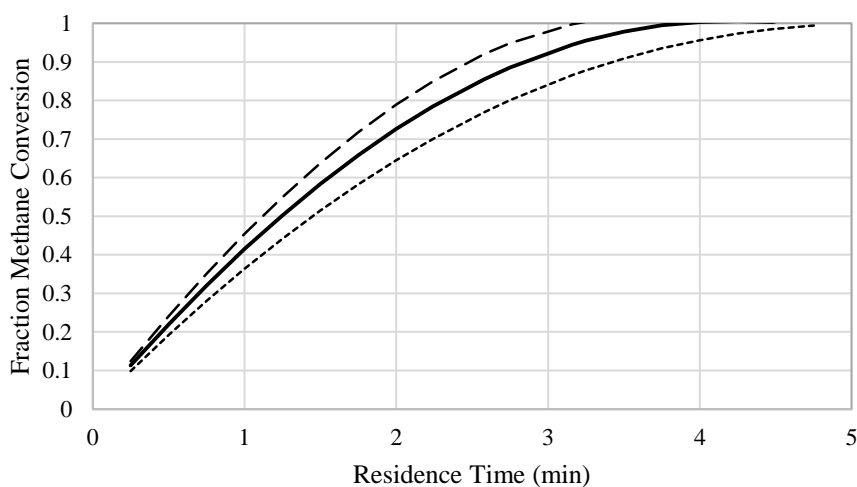
Figure 19. Parameter sensitivity analysis for the half saturation coefficient for a standard 5GB1 packed column. A standard value of 1.9 mg/mL (—) is compared to a double (- - - -) and half (– – –) that value.

A sensitivity analysis was then performed on the diffusion coefficient. For all previous modeling, a value of 80% of the diffusion coefficient of methane into water was used (0.001 cm^2/min) (Witherspoon & Saraf). A comparison of 100% and 25% of the coefficient was conducted holding all other parameters constant. The results are shown in *Figure 20.* Decreasing the D_f value resulted in a decrease in extent of methane consumed. This is expected because diffusion control transport into the biofilm. The results illustrate the importance of having a high diffusion coefficient in the alginate and agarose gels.
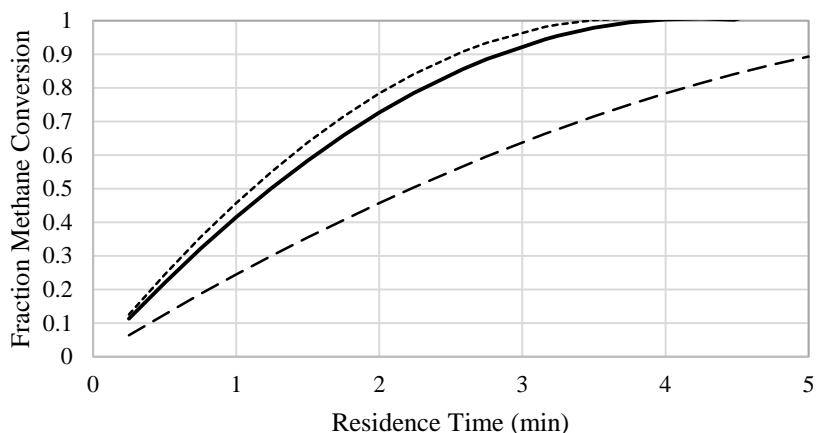
Figure 20. Parameter sensitivity analysis for the diffusion coefficient for a standard 5GB1 packed column. The standard value (▬) is compared to 1.0 D_f (- - - -) and 0.25 D_f (– – –).

The final parameter altered was influent substrate concentration. The experimental range used was 7.2 and 7.9 mg/mL, so an increase to 20 mg/mL and decrease to 1 mg/mL were analyzed holding all other parameters constant. *Figure 21* shows the comparison at all three substrate values. Increasing substrate concentration lowers the fraction of methane conversion. However at a residence time of 2.2 min, 50% of 20 mg CH_4/mL representing 10 mg CH_4/mL. At this same residence time, 83% of 1 mg CH_4/mL is consumed (0.83 mg CH_4/mL). There is a greater total mass consumed at the higher substrate concentration.
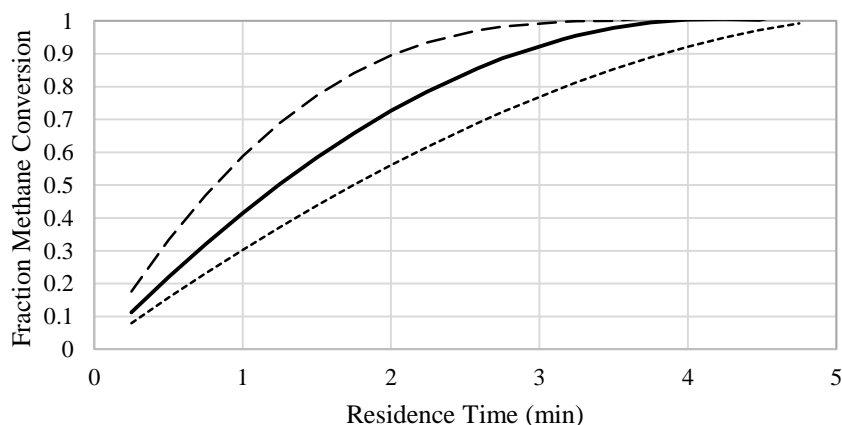
Figure 21. Parameter sensitivity analysis for influent substrate concentration for a standard 5GB1 packed column. A standard value of 7.7 mg/mL (▬) is compared to a value 20 mg/mL (- - - -) and 1 mg/mL (– – –).

All three parameters have varying degrees of effect on the theoretical methane consumption of 5GB1 in a packed column. Combinations of the best and worst case scenarios for each altered parameter are shown in *Figure 22*. The parameters for best methane removal were an increased D_f, decreased K_s, and decreased S_s. Overall, the sensitivity analysis demonstrated how changes in parameters can greatly influence the extent of methane consumption in a packed column.
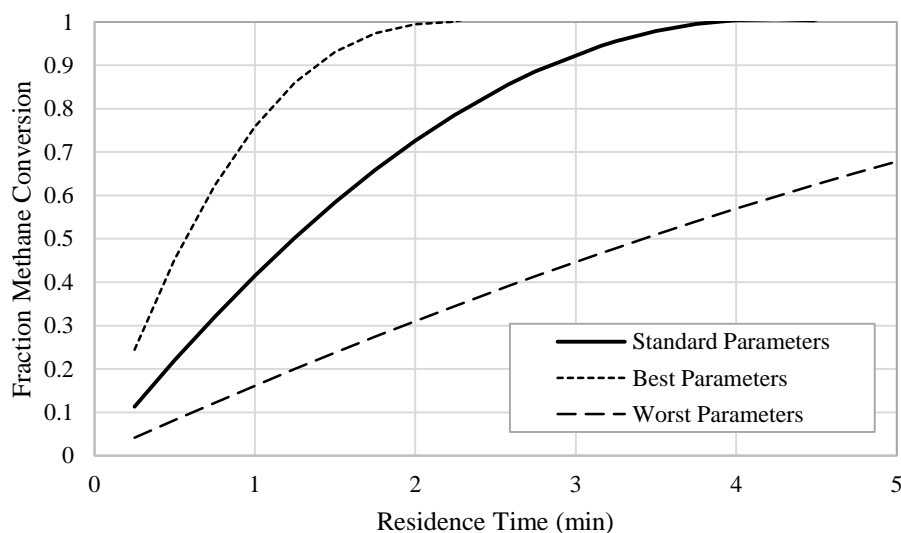
Figure 22. Parameter sensitivity testing comparing standard parameters (━) to the best (- - - -) and worst (– – –) case scenarios when adjusting substrate concentration, diffusion coefficient, and half saturation coefficient.

4.1.2.iv. Model parameter effects

For a more thorough understanding of protein effects on consumption, residence times for the 75% removal of methane were plotted versus protein concentration. Packed column experimental values for OB3b and 5GB1 are shown in *Figure 23*. Experimental values close to 75% (72-78%) are plotted.
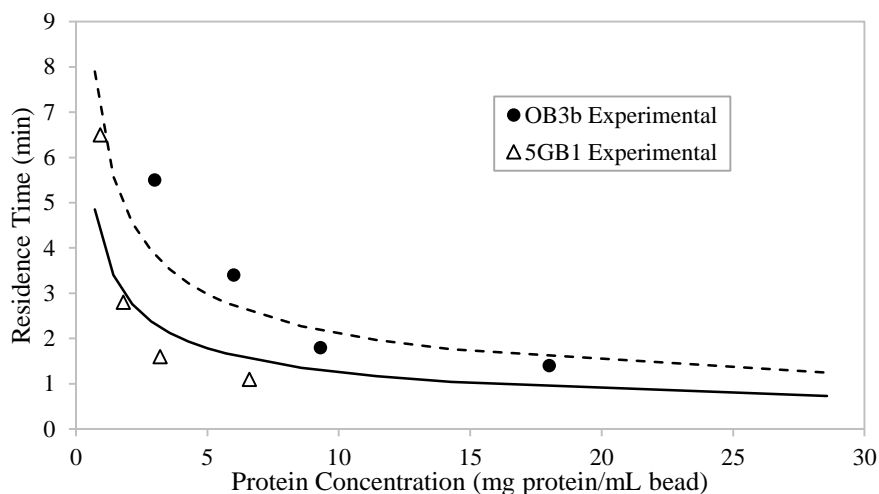
Figure 23. Residence time required for 75% removal of methane as a function of protein concentration. CMBR model outputs for OB3b (- - - -) and for 5GB1 (━) at 0.75 consumption. Experimental points for OB3b (●) and 5GB1 (Δ) represent the protein concentration and residence time for 75% removal.

Results show as protein concentration increases, the decreases in residence time changes more gradually. The long tail of the curve demonstrates the diminishing return on the increasing protein concentrations in the gel beads. The curves can be used to apply to future reactor designs, allowing optimal biomass concentrations to be selected to attain desired methane removal. Experimental values trends are consistent with model simulation.

4.1.3. BLP model comparison

The BLP reactor is a thin film micro-reactor to be used moving forward with this project. The 3 CMBR biofilm model was used to predict theoretical BLP behavior. The base case parameters used previously for the sensitivity analysis were applied for the comparison. Three process differences between the BLP and the packed column reactor are the geometry of the biofilm/gel beads, volume of the reactor, and the influent substrate concentrations. Input parameters for the base case and BLP case are shown in the section A12 in the appendix. The BLP is a thin film

reactor with a very high surface area/volume ratio, especially when compared to the gel beads. The specific area term, *a*, in the CMBR model is calculated by gel surface area/gel volume. So, the BLP has an increased *a* value. The BLP will have a two phase influent stream with methane and oxygen bubbles directly supplied to the media, providing an increased substrate concentration. However, the case modeled here is for an all liquid system. To mimic the gas and liquid aspect, the methane concentration was increased for the simulation to 14 mg CH4/mL. The standard packed column CMBR model output is compared to the BLP parameters in *Figure 24.* Another significant difference between the BLP and the CMBR is the determination of residence time. The BLP has a void volume of almost half of the total reactor volume, whereas the CMBR has a small fraction of the total reactor volume as void volume.

Results indicate an increased specific surface area increases the methane consumption. A theoretical higher surface area/volume ratio provided increased access to the available substrate allowing a higher concentration to be converted. The results indicate that the improved thin film reactor system should provide a significant increase in extent of methane production, ideal for high product formation.
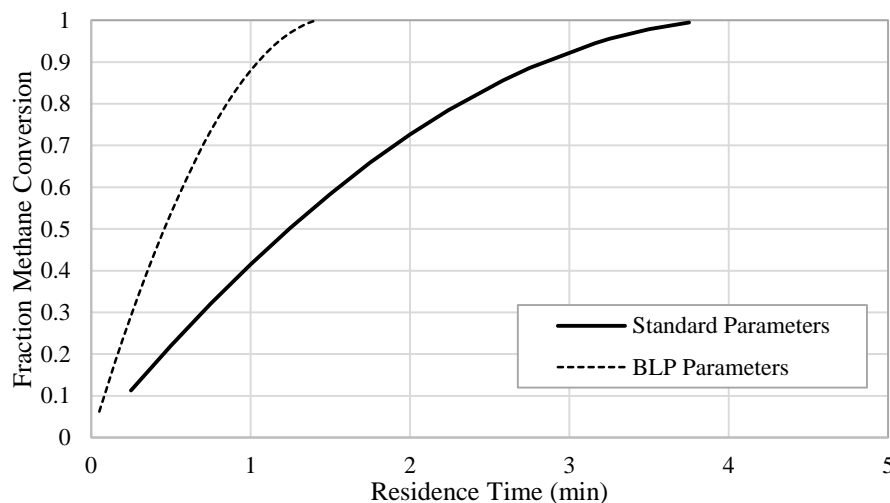
Figure 24. BLP modeling comparison for standard parameters (━) and the BLP parameters (- - - -). The specific surface area *a* and the influent substrate concentrations were altered to align with BLP process specifications.

4.1.4. Packed column summary

Overall, methanotrophic cultures in immobilized gels retained a high level of activity when placed in a packed column. Once in a packed column, the methanotrophic activity becomes dependent on residence time, biomass concentration, substrate concentration, and diffusion into the beads. A biofilm model of 3 CMBRs in series can simulate well the methane consumption seen in the column. Trends caused by increasing protein concentrations were well simulated. When comparing the two types of methanotrophic cultures, 5GB1 exhibited an average substrate utilization rate, K_{max}, of 0.0093 mg CH_4/mg protein/min while OB3b achieved 0.0089 mg CH_4/mg protein/min. Although the increase in activity was seen in batch reactors, the 5GB1 showed a higher level of performance for more than that reason alone. The decreased K_s, increased total volume of beads packed, and change in the residence time all contributed to the improvements in the experimental and model results.

The biofilm model simulated the methane consumption results of immobilized OB3b and 5GB1 using the rate constants determined in batch testing. Results of the sensitivity analysis found diffusion into the biofilm plays a significant role in methane removal. Increasing protein concentration displayed decreased required residence times for equal amounts of removal. Activity curves like that shown in *Figure 23* can be used to evaluate the behavior in reactors for desired substrate conversion.

SECTION 2

4.2. External and internal gelation for OB3b alginate beads

An alternative method for preparing alginate beads was investigated for simplification of the cross-linking process. This alternative was internal gelation. Gel beads were made using the previously discussed external cross-linking and internal gelation methods (Method #1 and Method #2) for comparison to suspended activity to determine the method viability.

4.2.1. Suspended vs. internal gelation vs. external gelation

Cell activity was evaluated for OB3b by measuring rates of ethylene epoxidation to ethylene oxide (ETO). Cultures in 70 mL vials were prepared for ethylene oxide (ETO) production with suspended and immobilized cultures (both internally or externally gelated using Method #1). Total protein concentrations ranged from 0.5 to 1.0 mg protein/mL bead. Ethylene was added to each vial and production of ETO was measured. *Figure 25 (left)* shows the resulting ETO production rates. The suspended and externally gelated cultures have comparable ETO production rates, whereas the internally gelated cultures showed very little ETO production. The

experiment was repeated three times to ensure no procedural errors caused the limited

activity. For all three experiments, the internally gelated culture exhibited nearly no

ETO production. ETO measurements are represented in peak area because an ETO

standard was not available to construct a standard curve.
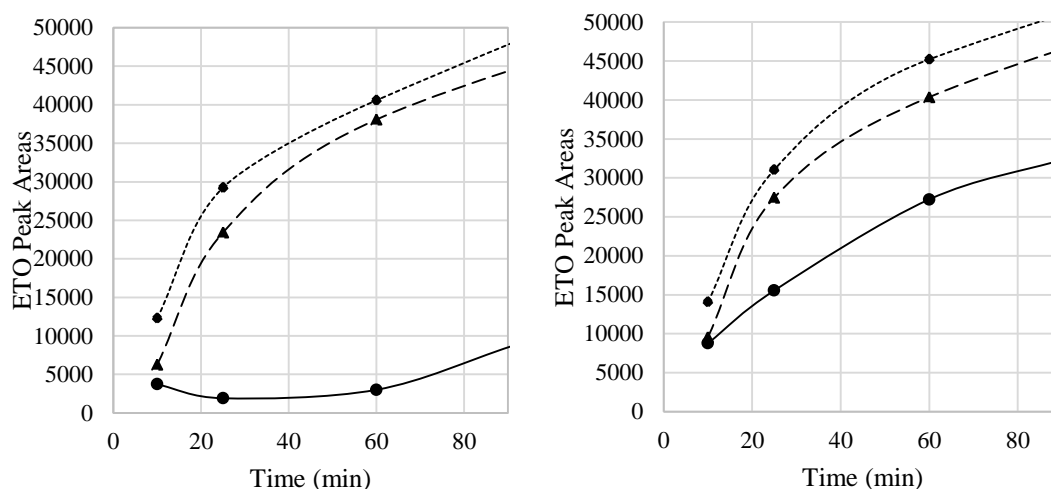
Figure 25. ETO production for OB3b suspended (♦), externally gelated (▲), and internally gelated (●) using Method #1 (left). ETO production is represented as a peak area from the GC measurements because no standard curve was created. ETO production experiment using Method #2 (right) with the same legend.

Further investigation of the internal gelation method indicated that the culture

was being exposed to a low pH when mixed with the glucono-δ-lactone solution,

which likely led to cell death. The method was altered to eliminate this issue through

buffering the GDL solution prior to culture addition, referred to as Method #2

(described previously). The same ETO production experiment at comparable protein

concentrations (0.5-1.0 mg protein/mL bead) with beads was conducted using Method

#2. *Figure 25 (right)* shows the results for ETO production with Method #2 for cell

immobilization. The internal gelation method continued to exhibit a much lower

activity than external gelation. Decreased activity in this form might be attributed to

an unknown oxygen demand on the culture or calcium carbonate and GDL enzyme

inhibitions. No further investigations were conducted on the internally gelated method and efforts shifted to 5GB1 testing in agarose beads.

4.2.2. Internal gelation summary

All internal gelation experiments displayed lowered activity compared to externally cross-linked cultures. Externally gelated cultures exhibited ETO production rates similar to suspended cultures, indicating diffusion into the gel beads was not severely limiting the culture activity. Internal gelation immobilization was abandoned and external cross-linking alginate and low melt agarose were selected as the most viable immobilization methods tested thus far.

SECTION 3

4.3. Production of methanol through inhibition of the OB3b MDH enzyme

The MDH enzyme in OB3b can produce methanol when chemically inhibited by cyclopropane or cyclopropanol. When cyclopropane is used, it is cometabolized to cyclopropanol by the sMMO enzyme, and the produced cyclopropanol inhibits the MDH enzyme, permitting methanol to accumulate. Investigations to determine if the inhibition is permanent, effective, and time dependent were conducted in batch and the packed column reactor.

4.3.1. Sequencing batch reactor – methanol production

Chemical inhibition of OB3b for methanol production was achieved through exposure to cyclopropane or cyclopropanol. A sequencing batch reactor was used for initial inhibition testing. OB3b immobilized in alginate beads was placed in a batch reactor with fresh media and was exposed to 100 µM cyclopropane for 2, 6, and 18

hours. The batch reactors were shaken at 300 rpm for the duration of the exposure. During this exposure period, the cells were oxidizing the cyclopropane to cyclopropanol using the MMO enzyme. So, after each inhibition time period, the cultures were rinsed with fresh media to remove any remaining cyclopropane or cyclopropanol. Fresh media was then added to the vials and 3 mL of methane was added to the headspace, and methanol production was measured. 100 µL headspace samples were obtained to measure methane concentration and 2 µL of liquid sample were used to measure methanol concentrations on the GC.

The methanol production was monitored over a 24 hour period and after methanol production ceased the beads were rinsed three times with DI water, and a new dose of methane was added to each reactor. Headspace and liquid samples were taken for the duration of methanol production. This process was repeated for 4 days. Comparisons of the methanol production for different exposure times are shown in *Figure 26.*

The highest levels of methanol production efficiency were observed on Day 1 of the experiment. Mass balances found 13-17% of the methane was consumed and was converted to methanol. As time proceeded lower levels of methane production were observed. In *Figure 27* the cumulative methanol production from this experiment is shown. The rinsing of the beads may have resulted in an unknown amount of the methanol being lost. A low concentration of the methanol could have leached out of the beads over time as was observed in the packed column test shown in *Figure 36* in the Appendix. This could indicate that the methanol was produced on only the first day of inhibition. Overall, the most effective exposure time was the 6

hour inhibition. Methane consumption was constant through each day of the

inhibition. Initial and final methane concentrations were measured every day *Figure 27* for the 6 hour exposure time and are shown in.
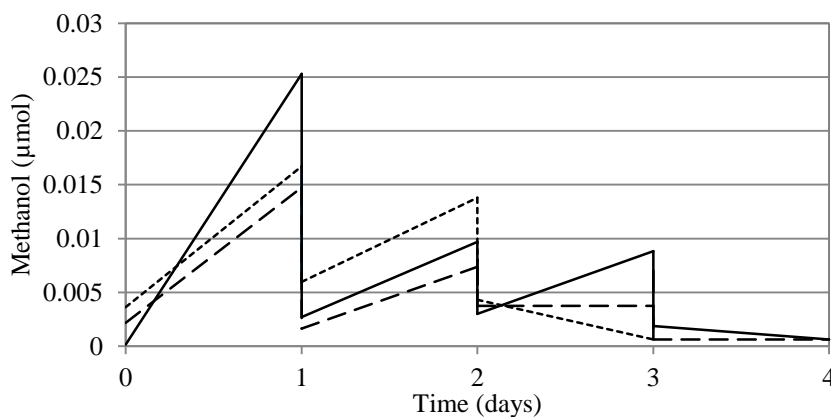
Figure 26. Methanol production from OB3b inhibited with cyclopropanol at 2 (······), 6 (▬), and 18 hour (- - - - -) exposure times. Methanol rinsed every day and fresh methane added for methanol production cycle.
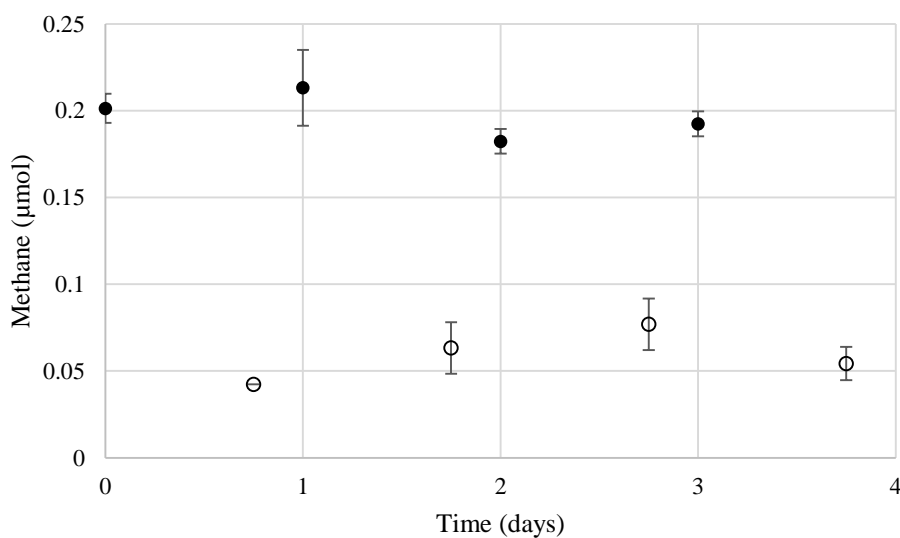
Figure 27. Initial methane (●) and final methane (○) as a function of time. Methane consumption remains constant throughout the entirety of the methanol production phase.

Results indicate that increased lengths of inhibition did not harm the culture.

However, the 6 hour exposure produced the higher concentrations of methanol. While

the effectiveness of cyclopropane inhibition decreased with time, the cultures did not lose MMO activity within 4 days (shown in *Figure 27*).
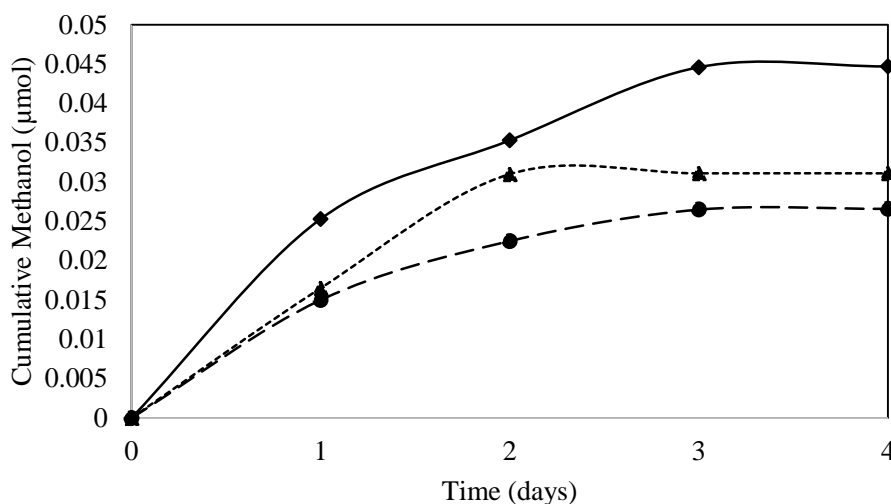
Figure 28. Cumulative methanol production from immobilized OB3b inhibited with cyclopropanol at 2 (···▲···), 6 (-♦-), and 18 hour (- -● - -) exposure times. Methanol rinsed every day and fresh methane was added for a methanol production cycle.

4.3.2. Packed column – methanol production

Methanol production in the continuous flow packed column was also evaluated. The column reactor provides constant flushing, control over flow rates and desired residence times, and continuous product removal. Comparison of the sequencing batch and a packed column reactors can indicate if more efficient methanol production can be achieved using a continuous flow column. OB3b was immobilized in alginate beads and packed into the up-flow column at a protein concentration of 10 mg protein/mL bead as previously described. Methane and oxygen saturated media were mixed at a 1:2 ratio and passed through the column to measure initial methane consumption activity before the inhibition phase.

Inhibition was achieved by filling syringe with a concentration of 500 µM biologically produced cyclopropanol in media and passed through the column for 3 pore volumes using a syringe pump. The flow was then stopped for 18 hours,

allowing long term exposure to cyclopropanol. The column was then flushed using

fresh media until no cyclopropanol remained as indicated by GC measurements. The

media containing dissolved methane and oxygen were passed through the column

using a peristaltic pump. Methane concentrations in the influent and effluent were

then measured using 1 mL samples, with 2 µL aqueous sample injected on the GC.

After methanol production slowed, the column was flushed and re-inhibited using the

same procedure previously described. The column was inhibited again for 18 hours,

and methanol production was monitored.

The methane and methanol concentrations are shown for the duration of the

experiment in *Figure 29* as consumption and production values. Each point represents

an average of triplicate measurements taken after steady state was reached.
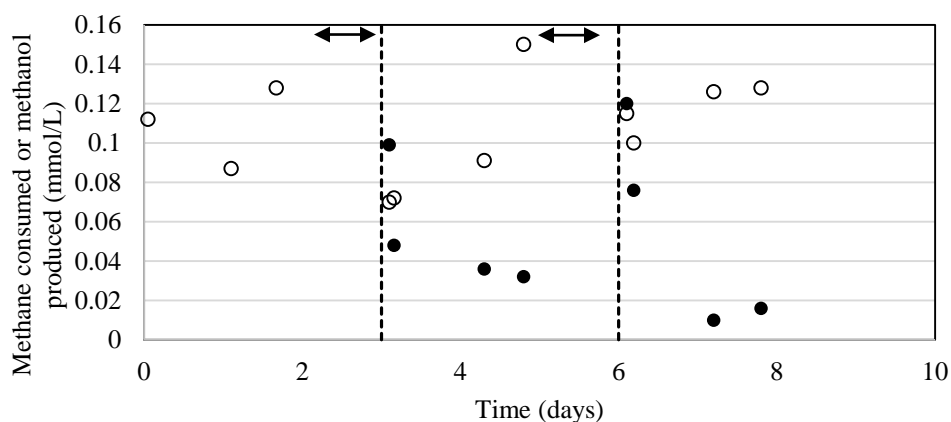
Figure 29. Methanol production in a packed column with OB3b immobilized in alginate at 10 mg protein/ mL bead. Total methane consumed (○) and methanol produced (●) concentrations plotted as a function of time. Inhibition cycles took place for 18 hours during the time marked (↔), column was flushed with fresh media at time marked by vertical dashed lines.

Methane consumption levels remained constant through the 8 day experiment

and methanol production was repeatable through two cycles of inhibition. Maximum

methanol concentrations of 0.1 mM were achieved and concentration slowly declined

as the inhibition effects lessened. Methanol production efficiency was calculated using a carbon balance on the influent and effluent of the system. Resulting maximum efficiencies were 75-140% (methanol produced/methane consumed) for both inhibition cycles indicating that nearly all of the methane consumed was converted to methanol. Methanol production efficiency variations occurred from methanol retardation in the packed column which slows the release of the methanol product. Methanol retardation effects were measures in a separate experiment shown in the appendix (*Figure 36*). Increased levels of methanol production compared to the sequencing batch test may be attributed to higher substrate influent concentration, continuous flow nature of the packed column, and different inhibiting compounds. Methanol was also likely lost in the washing steps that were performed in the sequencing batch tests.

4.3.3. Modeling of inhibited packed column

The methane consumption data obtained from the methanol production packed column experiment was simulated using 3 CMBRs in series model with biofilm diffusion and kinetics. The kinetic parameters used in the model are the same as used previously for OB3b immobilized in alginate (K_{max} = 0.0089 mg CH$_4$/mg protein/min and K_s = 0.0023 mg CH$_4$/mL). System parameters for the substrate concentration and flow rates were aligned with experimental parameters, and 80% of the diffusion coefficient for methane in water was used. Total protein concentration in the packed column was 10 mg protein/mL bead.

Experimental data from the packed column for methanol production and model simulation results are shown in *Figure 30.* Methane consumption

measurements plotted are as follows: before the first inhibition cycle (1), immediately

after the first inhibition during initial methanol production (2), at the end of the first

inhibition (3), immediately after the second inhibition during initial methanol

production (4), and at the end of the second inhibition (5). These points are shown in

the following figure.
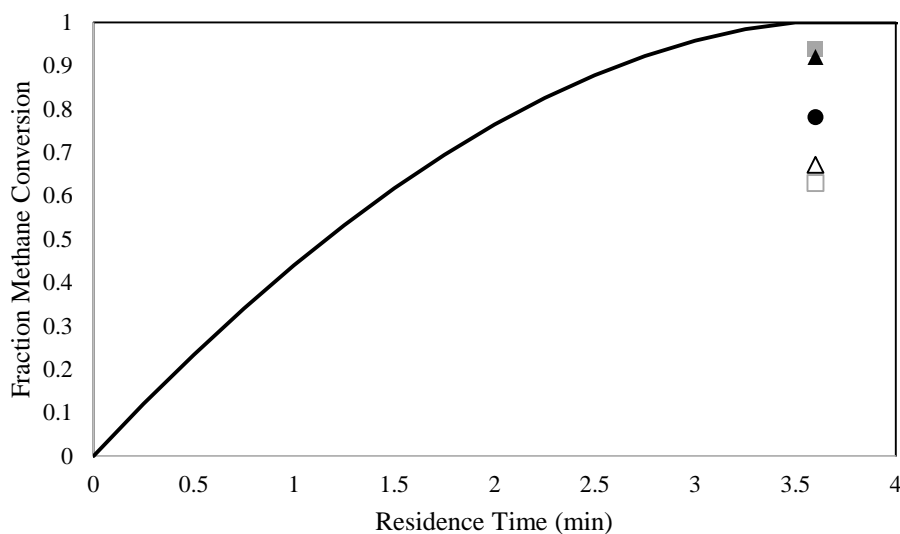
(●) Measurement 1 (Δ) Measurement 2 (▲) Measurement 3 (□) Measurement 4 (▪) Measurement 5

Figure 30. Fraction of methane consumption in the inhibited packed column. Measurements represent before the first inhibition cycle (●), immediately after the first inhibition (Δ), at the end of the first inhibition (▲), immediately after the second inhibition (□), and at the end of the second inhibition (▪).

Methane consumption decreased by 16% during the initial methanol

production periods, but increased by 18% toward the end of the inhibition phase.

Verifying that inhibition cyclopropanol does not significantly slow the long term

activity of the MMO enzyme. Repeated inhibition cycles also have no effect on the

consumption of methane by the MMO enzyme. The highest activity is in the ranges

achieved in the model simulation.

4.3.4. Methanol production summary

OB3b immobilized in alginate gel beads produced methanol in both batch and continuous reactors through MDH chemical inhibition by cyclopropanol and cyclopropane. Efficiencies ranged from 13-17% in the sequencing batch reactor and 75-140% in the packed column reactor. The differences in these efficiencies are likely due to constant methanol flushing in the packed column, increased substrate concentrations, and different inhibiting compounds (purchased cyclopropane and biologically produced cyclopropanol).

CHAPTER 5
DISCUSSION

The methanotrophic cultures investigated in this study, OB3b and 5GB1, showed promising substrate utilization rates in both suspended and immobilized forms. A slight decrease in activity was seen with immobilized culture compared to suspension, however the decrease was not significant. Immobilization of cultures has been implemented in the pharmaceutical and food industries and for heavy metal removal (Li et al., 1996; Narayanan et al., 2006). However, microbes are not as commonly immobilized due to potential mass transfer limitations and inability for the culture to grow. Immobilization effects on microbes are unpredictable and dependent on a number of factors. Kourkoutas et al. (2004) reviewed a number of immobilization investigations on microbial activity and the benefits were as follows: higher concentrations of biomass, increased synthesis of enzymes when compared to free cells, and increased yield of product formed. However, for this investigation the comparison of free and immobilized activities showed no significant increase or decrease in activity. However, high biomass concentrations were easily achieved using the immobilization method.

When comparing the two cultures 5GB1 exhibited slightly higher rates of substrate utilization in all reactor settings. OB3b maximum substrate utilization rates from literature (Lee et al., 2006) are 0.011 mg CH_4/mg protein/min and experimental values fall near this value with an average rate of 0.0089 mg CH_4/mg protein/min. 5GB1 performed at slightly higher rates of 0.0093 mg CH_4/mg protein/min.

Applying these rates to the model developed by Rittmann and McCarty provided insight into immobilized microbial trends. The model has previously been used to understand system behavior for naturally formed biofilms. Application of the model to the methanotroph packed column systems embodies the behavior of the cultures well. The model provided a good fit to the experimental packed column results through applying a diffusion coefficient of 80% of the diffusion coefficient of methane in water along with independently derived kinetic parameters. Experimental trends were well represented by the model, with no fitting of parameters necessary. Results from experiment and model predictions indicate an increase in protein led to a decreased residence time required for a constant methane removal. However, mass transfer and kinetic restrictions resulted in a limitation on protein concentrations increasing performance.

Methanotrophs have recently been under investigation for methane conversion to a usable product. ARPA-E is a program of the Department of Energy is currently funding research on this topic in hopes of finding a low capital cost microbial process (Haynes & Gonzalez, 2014). Current investigations for methane removal include separation and concentration of biocatalysts from organisms for cell free conversion, methylation using methanotrophs, and high efficiency conversions using zeolite catalysts. Chemically inhibiting methanotrophs for methanol production is also under investigation. Our results indicate methanol production through chemical inhibition of MDH is possible. Our initial test in the continuous flow column shows methanol production was short lived and re-inhibition was required. Although OB3b is capable of producing methanol, there is great interest in producing a higher valued product.

Pursuit of genetic enhancement of 5GB1 for higher rates and valuable product production are underway. University of Washington and Rice University are investigating these possibilities. Although 5GB1 is not as widely investigated as OB3b, it provides a more viable option and activity enhancement methods should be further pursued. Our results demonstrate that 5GB1 can be effectively immobilized in agarose gels which can tolerate the high pH and salt concentrations required for optimal 5GB1 performance. Experimental methods and the model analysis developed in this project will be used in the testing of the modified strain of 5GB1.

CHAPTER 6
CONCLUSIONS AND FUTURE WORK

Main conclusions from this investigation of methanotrophs for the conversion

of methane to a usable product are listed below:

- Integrated Monod equations provides useful and accurate means of determining

  kinetic parameters from batch rate tests. Average kinetic parameters for cultures

  determined experimentally are shown in *Table 2* (repeated below). 5GB1 displays

  slightly increased rates of methane utilization than OB3b and the immobilized

  cultures exhibited significantly increased values of K_s.

Culture Type	K_s (mg CH_4/L)	K_{max} (mg CH_4/mg protein/min)
OB3b Suspended	2.3 ± 0.3 [a]	0.0089 ± 0.0009 [c]
OB3b Immobilized	3.4 ± 0.3 [b]	0.0085 ± 0.001 [c]
5GB1 Suspended	1.9 ± 0.2 [a]	0.0093 ± 0.004 [c]
5GB1 Immobilized	3.1 ± 0.4 [b]	0.0088 ± 0.001 [c]

- Immobilization method comparisons determined agarose and externally cross-

  linked Ca-alginate have comparable effects on activity. Packed column

  experiments with 3.3 mg OB3b/mL bead immobilized in alginate and 3.1 mg

  OB3b/mL bead in agarose showed equal levels of methane utilization. High

  microbial activity was achieved using both methods of immobilization.

- 3 CMBR model for biofilm reaction-diffusion developed by Rittmann and

  McCarty accurately describes the following trends seen in the packed column for

  both OB3b and 5GB1:

  o Protein increases led to decreased residence time requirement for methane

    utilization.

- o High levels of protein concentrations do not provide equally high levels of methane consumption. Thus, there are diminishing returns on increasing biomass concentration in the beads.

- o The diffusion coefficient and specific surface area of the biofilm significantly affect the outcome of the CMBR model. The sensitivity analysis determined an increased diffusion coefficient and decreased half saturation coefficient improved methane consumption. The thin film nature of the BLP reactor increased the access to substrate, improving overall methane consumption.

- Internal gelation is not a viable option for the methanotroph cultures because the exposure to the low pH of GDL harms the culture and significantly lowers ETO production levels. But Method #2 showed this could be partially overcome.

- Methanol can be produced by OB3b at measurable rates by chemical inhibition of MDH by cyclopropanol and cyclopropane. Batch and packed column reactors both displayed high levels of methanol production. Batch methanol production efficiencies ranged from 13-17% and packed column efficiencies ranged from 75-140%. Reasons for the increased efficiencies are due to constant product flushing, varying substrate concentration, and exposure to either purchased cyclopropane or biologically produced cyclopropanol.

Verification of kinetic parameters for OB3b and 5GB1 need to be conducted using more batch kinetic experiments at various substrate and protein concentrations. Investigation of a broader range of methane concentrations in the influent of the packed column should be conducted for better understanding of the BLP reactor

potential. The bead size in packed column should be altered to understand geometry effects on mass transfer within immobilized forms. An attempt should be made at inhibiting 5GB1 using cyclopropanol and cyclopropane to produce methanol.

Modification of the model used for simulation of the packed column and BLP reactor should be further investigated. Current modeling methods represent well the basic trends in parameter changes on substrate removal however, the project will soon be focusing on a thin film, two phase, high mass transfer reactor (Bio-Lamina Plate Reactor). This reactor will have two phases flowing through the system, so a model needs to be created to better represent the second phase.

Activity testing will need to be continued with the genetically modified 5GB1 culture. Experiments should be repeated to determine new kinetic parameters as well as study product formation in a beaded packed column.

Finally, the diffusion coefficient of methane and oxygen in the gels should be determined experimentally. There are estimations of this value in literature and they align with the experiments well, however an accurate representation of how the substrate diffuses into the gels would be very useful. The sensitivity analysis indicated that the diffusion coefficient had a significant impact on model output, measuring a value would be beneficial.

Overall, 5GB1 and OB3b demonstrate comparable methane removal rates in suspended and immobilized forms in batch and packed column reactors. Further investigation can be done to understand influent substrate concentration and two phase flow effects for determining optimal reactor settings for the BLP reactor.

BIBLIOGRAPHY

Aksu, Z., Egretli, G., & Kutsal, T. (1998). A comparative study of copper(II) biosorption on Ca-alginate, agarose and immobilized C. vulgaris in a packed-bed column. Process Biochemistry.

Anthony, C., & Williams, P. (2003). The structure and mechanism of methanol dehydrogenase. *Biochimica et Biophysica Acta (BBA) - Proteins and Proteomics*, *1647*(1-2), 18–23. http://doi.org/10.1016/S1570-9639(03)00042-6

Ca\-nizares, R. O., Dominguez, A. R., Rivas, L., Montes, M. C., Travieso, L., & Benetez, F. (1993). Free and immobilized cultures of Spirulina maxima for swine waste treatment. *Biotechnology Letters*, *15*(3), 321–326. http://doi.org/10.1007/BF00128327

Chang, H. T., & Rittmann, B. E. (1987). Mathematical modeling of biofilm on activated carbon. *Environmental Science & Technology*, *21*(3), 273–280.

Chan, L. W., Lee, H. Y., & Heng, P. W. S. (2002). Production of alginate microspheres by internal gelation using an emulsification method. *International Journal of Pharmaceutics*, *242*(1), 259–262.

Colby, J., Stirling, D. I., & Dalton, H. (1977). The soluble methane mono-oxygenase of Methylococcus capsulatus (Bath). Its ability to oxygenate n-alkanes, n-alkenes, ethers, and alicyclic, aromatic and heterocyclic compounds. *Biochemical Journal*, *165*(2), 395–402.

Duan, C., Luo, M., & Xing, X. (2011). High-rate conversion of methane to methanol by Methylosinus trichosporium OB3b. *Bioresource Technology*, *102*(15), 7349–7353. http://doi.org/10.1016/j.biortech.2011.04.096

Eller, G., Stubner, S., & Frenzel, P. (2001). Group-specific 16S rRNA targeted probes for the detection of type I and type II methanotrophs by fluorescence in situ hybridisation. *FEMS Microbiology Letters*, *198*(2), 91–97.

Fox, B. G., Borneman, J. G., Wackett, L. P., & Lipscomb, J. D. (1990). Haloalkene oxidation by the soluble methane monooxygenase from Methylosinus trichosporium OB3b: mechanistic and environmental implications. *Biochemistry*, *29*(27), 6419–6427.

Furuto, T., Takeguchi, M., & Okura, I. (1999). Semicontinuous methanol biosynthesis by Methylosinus trichosporium OB3b. *Journal of Molecular Catalysis A: Chemical*, *144*(2), 257–261.

Gilman, A., Laurens, L. M., Puri, A. W., Chu, F., Pienkos, P. T., & Lidstrom, M. E. (2015). Bioreactor performance parameters for an industrially-promising methanotroph Methylomicrobium buryatense 5GB1. *Microbial Cell Factories*, *14*(1). http://doi.org/10.1186/s12934-015-0372-8

Gonzalez, R., & Conrado, R. (2014). Envisioning the Bioconversion of Methane to Liquid Fuels. *Science*, *343*(6171), 620–621. http://doi.org/10.1126/science.1250214

Gornall, A. G., Bardawill, C. J., David, M. M., & others. (1949). Determination of serum proteins by means of the biuret reaction. *J. Biol. Chem*, *177*(2), 751–766.

Hakemian, A. S., & Rosenzweig, A. C. (2007). The Biochemistry of Methane Oxidation. *Annual Review of Biochemistry*, *76*(1), 223–241. http://doi.org/10.1146/annurev.biochem.76.061505.175355

Han, J.-S., Ahn, C.-M., Mahanty, B., & Kim, C.-G. (2013). Partial Oxidative Conversion of Methane to Methanol Through Selective Inhibition of Methanol Dehydrogenase in Methanotrophic Consortium from Landfill Cover Soil. *Applied Biochemistry and Biotechnology*, *171*(6), 1487–1499. http://doi.org/10.1007/s12010-013-0410-0

Hanson, R. S., & Hanson, T. E. (1996). Methanotrophic bacteria. *Microbiological Reviews*, *60*(2), 439–471.

Haynes, C. A., & Gonzalez, R. (2014). Rethinking biological activation of methane and conversion to liquid fuels. *Nature Chemical Biology*, *10*(5), 331–339. http://doi.org/10.1038/nchembio.1509

Hwang, I. Y., Lee, S. H., Choi, Y. S., Park, S. J., Na, J. G., Chang, I. S., … Lee, E. Y. (2014). Biocatalytic Conversion of Methane to Methanol as a Key Step for Development of Methane-Based Biorefineries. *Journal of Microbiology and Biotechnology*, *24*(12), 1597–1605. http://doi.org/10.4014/jmb.1407.07070

Jiang, H., Chen, Y., Jiang, P., Zhang, C., Smith, T. J., Murrell, J. C., & Xing, X.-H. (2010). Methanotrophs: Multifunctional bacteria with promising applications in environmental bioengineering. *Biochemical Engineering Journal*, *49*(3), 277–288. http://doi.org/10.1016/j.bej.2010.01.003

Kaluzhnaya, M., & Khmelenina, V. (2001). Taxonomic Characterization of New Alkaliphilic and Alkalitolerant Methanotrophs from Soda Lakes of the Southeastern Transbaikal Region and description of Methylomicrobium buryatense sp.nov. Systematic and Applied Microbiology.

Kalyuzhnaya, M. G., Hristova, K. R., Lidstrom, M. E., & Chistoserdova, L. (2008). Characterization of a Novel Methanol Dehydrogenase in Representatives of Burkholderiales: Implications for Environmental Detection of Methylotrophy and Evidence for Convergent Evolution. *Journal of Bacteriology*, *190*(11), 3817–3823. http://doi.org/10.1128/JB.00180-08

Kohyama, K., Yoshida, M., & Nishinari, K. (1992). Rheological study on gelation of soybean 11S protein by glucono-. delta.-lactone. *Journal of Agricultural and Food Chemistry*, *40*(5), 740–744.

Kostov, G., Popova, S., Gochev, V., Koprinkova-Hristova, P., Angelov, M., & Georgieva, A. (2012). Modeling of Batch Alcohol Fermentation with Free and Immobilized Yeasts *Saccharomyces Cerevisiae* 46 EVD. *Biotechnology & Biotechnological Equipment*, *26*(3), 3021–3030. http://doi.org/10.5504/BBEQ.2012.0025

Kourkoutas, Y., Bekatorou, A., Banat, I. ., Marchant, R., & Koutinas, A. . (2004). Immobilization technologies and support materials suitable in alcohol beverages production: a review. *Food Microbiology*, *21*(4), 377–397. http://doi.org/10.1016/j.fm.2003.10.005

Lee, S. G., Goo, J. H., Kim, H. G., Oh, J.-I., Kim, Y. M., & Kim, S. W. (2004). Optimization of methanol biosynthesis from methane using Methylosinus trichosporium OB3b. *Biotechnology Letters*, *26*(11), 947–950.

Lee, S.-W., Keeney, D. R., Lim, D.-H., Dispirito, A. A., & Semrau, J. D. (2006). Mixed Pollutant Degradation by Methylosinus trichosporium OB3b Expressing either Soluble or Particulate Methane Monooxygenase: Can the Tortoise Beat the Hare? *Applied and Environmental Microbiology*, *72*(12), 7503–7509. http://doi.org/10.1128/AEM.01604-06

Li, R. H., Altreuter, D. H., & Gentile, F. T. (1996). Transport characterization of hydrogel matrices for cell encapsulation. *Biotechnology and Bioengineering*, *50*(4), 365–373.

Murrell, J. C., McDonald, I. R., & Gilbert, B. (2008). Regulation of expression of methane monooxygenases by copper ions. Trends in Microbiology.

Myhre, G., & Shindell, D. (2013). Climate Change 2013: The Physical Science Basis - Anthropogenic and Natural Radiative Forcing Supplementary Material. Cambridge University Press.

Narayanan, J., Xiong, J.-Y., & Liu, X.-Y. (2006). Determination of agarose gel pore size: Absorbance measurements vis a vis other techniques. *Journal of Physics: Conference Series*, *28*, 83–86. http://doi.org/10.1088/1742-6596/28/1/017

Obuekwe, C. O., & Al-Muttawa, E. M. (2001). Self-immobilized bacterial cultures with potential for application as ready-to-use seeds for petroleum bioremediation. *Biotechnology Letters*, *23*(13), 1025–1032.

Overview of Greenhouse Gases. (2016, March). *United States EPA*.

Patel, R. N., Hou, C. T., Laskin, A. I., & Felix, A. (1982). Microbial oxidation of hydrocarbons: properties of a soluble methane monooxygenase from a facultative methane-utilizing organism, Methylobacterium sp. strain CRL-26. *Applied and Environmental Microbiology*, *44*(5), 1130–1137.

Plessas, S., Bekatorou, A., Koutinas, A., Soupioni, M., Banat, I., & Marchant, R. (2007). Use of Saccharomyces cerevisiae cells immobilized on orange peel as biocatalyst for alcoholic fermentation. *Bioresource Technology*, *98*(4), 860–865. http://doi.org/10.1016/j.biortech.2006.03.014

Rittmann, B. E., & McCarty, P. L. (2001). Environmental biotechnology: principles and applications. McGraw-Hill.

Shimoda, M., & Okura, I. (1990). Effect of cyclopropane treatment of Methylosinus trichosporium (OB3b) for methane hydroxylation. *Journal of the Chemical Society, Chemical Communications*, (7), 533–534.

Shimomura, T., Suda, F., Uchiyama, H., & Yag, O. (1997). Biodegradation of trichloroethylene by methylocystis sp. Strain m immobilized in gel beads in a fluidized-bed bioreactor. Water Research.

Smith, L. H., & McCarty, P. L. (1997). Laboratory evaluation of a two-stage treatment system for TCE cometabolism by a methane-oxidizing mixed culture. *Biotechnology and Bioengineering*, *55*(4), 650–659.

Smith, L. H., McCarty, P. L., & Kitanidis, P. K. (1998, June). Spreadsheet Method for Evaluation of Biochemical Reaction Rate Coefficients and Their Uncertainties by Weighted Nonlinear Least-Squares Analysis of the Integrated Monod Equation. Applied Enrionmental Microbiology.

Speitel Jr, G. E., & McLay, D. S. (1993). Biofilm reactors for treatment of gas streams containing chlorinated solvents. *Journal of Environmental Engineering*, *119*(4), 658–678.

Steinbüchel, A. (Ed.). (2005). *Polysaccharides and polyamides in the food industry: properties, production, and patents*. Weinheim: Wiley.

Tsezos, M., & Deutschmann, A. A. (1990). An investigation of engineering parameters for the use of immobilized biomass particles in biosorption. *Journal of Chemical Technology and Biotechnology*, *48*(1), 29–39.

Tsezos, M., & Deutschmann, A. A. (1992). The use of a mathematical model for the study of the important parameters in immobilized biomass biosorption. *Journal of Chemical Technology and Biotechnology*, *53*(1), 1–12.

Uchiyama, H., Oguri, K., Nishibayashi, M., Kokufuta, E., & Yagi, O. (1995). Trichloroethylene Degradation by Cells of a Methane-Utilizing Bacterium, Metylocystis sp. M, Immobilized in Calcium Alginate. Journal of Fermentation and Bioengineering.

Usha, S., Anitha, S., & Rajendran, L. (2012). Approximate analytical solution of non-linear reaction diffusion equation in fluidized bed biofilm reactor. *Natural Science*, *04*(12), 983–991. http://doi.org/10.4236/ns.2012.412127

APPENDIX

A1. Media recipes for OB3b and 5GB1.

<u>**OB3b**</u>

To make 1L solution:

1 L nanopure DI water
1 g KNO3
1 g MgSO4*7H2O
0.134 g CaCl2*2H20
1 g KNO3

Autoclave for 30-45 minutes
When temperature has decreased to
room temperature add:

0.7 g Na2HPO4*7H2O
2 mL trace element solution

Trace element solution:

1 L nanopure DI water
1.29 g Na2EDTA
1.69 g FeSO4*7H2O
0.8 g ZnSO4*7H2O
0.005 g MnCl2*2H2O
0.03 g H3BO3
0.05 g CoCl2*6H2O
0.002 g NiCl2*6H2O
0.05 g Na2MoO4*2H2O
0.75 g CuCl2*2H2O

<u>**5GB1**</u>

To make 1L solution:

1 L nanopure DI water
7.5 g NaCl
0.2 g MgSO4*7H2O
0.014 g CaCl2*2H20
1 g KNO3

Divide into 150 mL bottles
Autoclave for 30-45 minutes
When temperature has decreased to
room temperature add:

**Before use add to each 150 mL
bottle:**
7.5 mL 1M carbonate buffer
3 mL phosphate buffer
0.3 mL trace elements solution

A2. Example of peristaltic pump calibration for flow rates through packed column.

Triplicate measurements were timed to verify accurate flow rates for each experiment

(shown in *Table 4*). *Figure 31* shows flow rates as a function of pump setting to find

the best fit line used in flow rate conversion. This procedure was followed before

each column experiment.

Table 4. Pump calibration example. Measuring the time to flow 5 mL of media through the column is used for flow rate estimates.

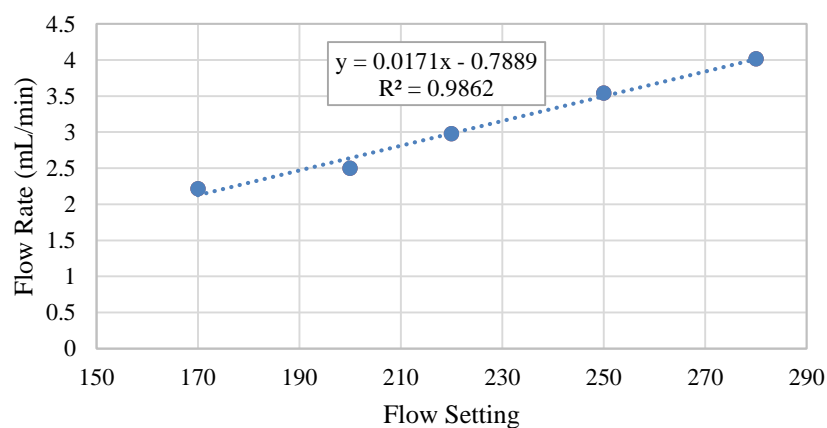| Flow Setting	Time for 5 mL Effluent (s)	Average Flow Rate (mL/min)
170	135	**2.22**
	133	
	138	
200	125	**2.50**
	117	
	118	
220	98	**2.98**
	94	
	110	
250	81	**3.54**
	86	
	87	
280	67	**4.02**
	75	
	82	

Figure 31. Pump calibration for accurate flow measurements. Equation represents the best fit line used for pump setting conversions to flow rate.

A3. Example of gas chromatograph injections and conversions to aqueous and headspace concentrations. *Table 5* showing the volume of methane added, total moles, aqueous concentration, gas concentration, and peak areas measured on the GC. *Figure 32* displaying the plot of peak area as a function of concentrations for simple conversions between peak area and concentrations.

Table 5. Calibration values for methane GC concentration measurements. Headspace injections on the GC converted from peak area (PA) to liquid concentration in the batch vial using the Henry's Law Constant. *Figure 31* shows plot of results to obtain the standard curve.

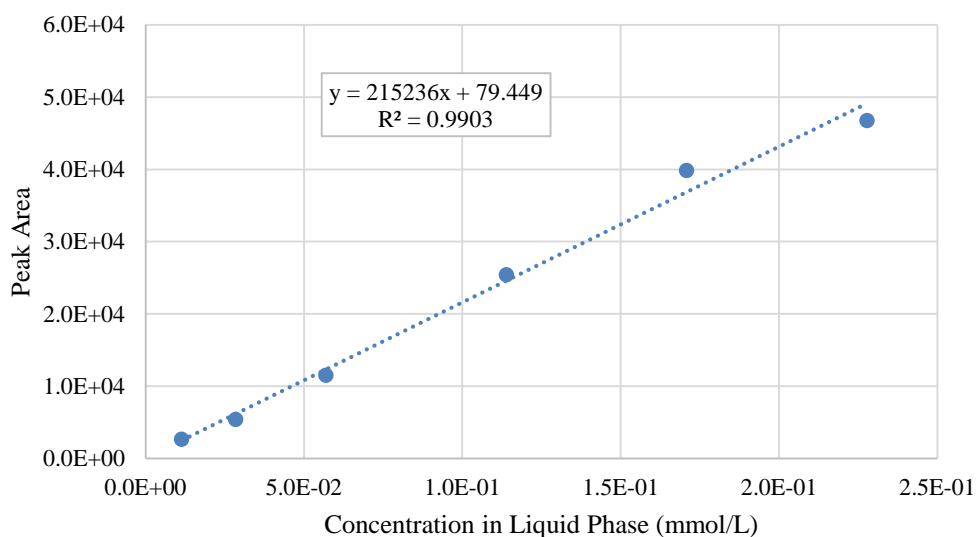| Volume CH$_4$ (mL CH$_4$)	(L CH$_4$)	Total Moles CH$_4$	Cg	Cw	Total Mole Check	Cw	PA Average
0.2	0.0002	8.9E-06	3.4E-04	1.1E-05	8.9E-06	1.1E-02	2.7E+03
0.5	0.0005	2.2E-05	8.5E-04	2.8E-05	2.2E-05	2.8E-02	5.4E+03
1	0.001	4.5E-05	1.7E-03	5.7E-05	4.5E-05	5.7E-02	1.2E+04
2	0.002	8.9E-05	3.4E-03	1.1E-04	8.9E-05	1.1E-01	2.5E+04
3	0.003	1.3E-04	5.1E-03	1.7E-04	1.3E-04	1.7E-01	4.0E+04
4	0.004	1.8E-04	6.8E-03	2.3E-04	1.8E-04	2.3E-01	4.7E+04

y = 215236x + 79.449
R² = 0.9903

Figure 32. Calibration curves for methane concentrations for headspace injections on the GC. Triplicate vials were prepared and averages were plotted for determination of the standard curve.

A4. Integrated Monod model derivation for batch testing. Methane consumption experimental data used with the integrated Monod curve to find the best fit kinetic parameters. Variable were all held constant except for the half saturation coefficient and the maximum substrate utilization rate. The final equation (*Equation 38*) was used in the solver method to find the best fit. The follow integration was completed to verify equations from the literature.

Monod equation for substrate utilization and cell growth:

$$-\frac{dC_L}{dt} = \frac{kC_LX_a}{k_s+C_L} \tag{20}$$

Input growth equation for bacterial growth with substrate consumption:

$$X_a = X_{a0} + Y(C_{L0} - C_L) \tag{21}$$

$$-\frac{dC_L}{dt} = \frac{kC_L(X_{a0}+Y(C_{L0}-C_L))}{k_s+C_L} \tag{22}$$

$$-\frac{dC_L}{dt}\frac{(k_s+C_L)}{C_L} = k(X_{a0} + Y(C_{L0} - C_L)) \tag{23}$$

$$-\frac{dC_L}{dt}\frac{(k_s+C_L)}{C_L(X_{a0}+Y(C_{L0}-C_L))} = k \tag{24}$$

$$dC_L\frac{(k_s+C_L)}{C_L(X_{a0}+Y(C_{L0}-C_L))} = -kdt \tag{25}$$

$$dC_L\left\{\frac{k_s}{C_LX_{a0}+C_LYC_{L0}-YC_L{}^2))} + \frac{C_L}{C_LX_{a0}+C_LYC_{L0}-YC_L{}^2))}\right\} = -kdt \tag{26}$$

$$dC_L\left\{\frac{k_s}{C_LX_{a0}+C_LYC_{L0}-YC_L{}^2))} + \frac{1}{X_{a0}+YC_{L0}-YC_L))}\right\} = -kdt \tag{27}$$

Integrated in sections (Terms 1, 2, and 3). Term 1:

$$= dC_L\left\{\frac{k_s}{C_LX_{a0}+C_LYC_{L0}-YC_L{}^2))}\right\} \tag{28}$$

$$= dC_L\left\{\frac{k_s}{C_L(X_{a0}+YC_{L0})-YC_L{}^2))}\right\} \tag{29}$$

Using the table of integration rule:

$$\int \left\{ \frac{k_s}{C_L(X_{a0}+YC_{L0})-YC_L{}^2))} \right\} dC_L = \frac{k_s}{X_{a0}+YC_{L0}} \ln \left\{ \frac{2(-Y)C_L+(X_{a0}+YC_{L0})-\sqrt{(X_{a0}+YC_{L0})^2}}{2(-Y)C_L+(X_{a0}+YC_{L0})+\sqrt{(X_{a0}+YC_{L0})^2}} \right\}$$

(30)

$$= \frac{k_s}{X_{a0}+YC_{L0}} \ln \left\{ \frac{2(-Y)C_L}{2(-Y)C_L+2X_{a0}+2YC_{L0})} \right\}$$

(31)

$$= \frac{k_s}{X_{a0}+YC_{L0}} \{\ln(-YC_L) - \ln(X_{a0}+Y(C_{L0}-C_L))\}$$

(32)

Term 2:

$$\int \left\{ \frac{1}{(X_{a0}+YC_{L0}-YC_L))} \right\} dC_L = -\frac{1}{Y}\ln(-YC_L+X_{a0}+YC_{L0}) + \frac{1}{Y}\ln(X_{a0})$$

(33)

$$= -\frac{1}{Y}\ln(X_{a0}+Y(C_{L0}-YC_L)) + \frac{1}{Y}\ln(X_{a0})$$

(34)

Term 3:

$$\int -kdt = -kt$$

(35)

Combination of terms:

$$\frac{k_s}{X_{a0}+YC_{L0}}\{\ln(-YC_L) - \ln(X_{a0}+Y(C_{L0}-C_L))\}\dots$$

$$\dots -\frac{1}{Y}\ln(X_{a0}+Y(C_{L0}-YC_L)) + \frac{1}{Y}\ln(X_{a0}) = -kt$$

(36)

$$t = -\frac{1}{k} \left\{ \begin{array}{c} \frac{-k_s}{X_{a0}+YC_{L0}}\ln(X_{a0}+Y(C_{L0}-C_L)) + \frac{-k_s}{X_{a0}+YC_{L0}}\ln\left(\frac{C_{L0}}{X_{a0}C_L}\right)\dots \\ \dots -\frac{1}{Y}\ln(X_{a0}+Y(C_{L0}-YC_L)) + \frac{1}{Y}\ln(X_{a0}) \end{array} \right\}$$

(37)

$$t = \frac{1}{k} \left\{ \begin{array}{c} \frac{k_s}{X_{a0}+YC_{L0}}\ln(X_{a0}+Y(C_{L0}-C_L)) + \frac{k_s}{X_{a0}+YC_{L0}}\ln\left(\frac{C_{L0}}{X_{a0}C_L}\right)\dots \\ \dots +\frac{1}{Y}\ln(X_{a0}+Y(C_{L0}-YC_L)) - \frac{1}{Y}\ln(X_{a0}) \end{array} \right\}$$

(38)

This final equation equals the integrated Monod curve used for modeling purposes.

The integrated Monod curve was used to find best fit kinetic parameters.

A5. $K_{max,app}$ derivation:

Original Monod Equation for 2-Phase System:

$$\frac{dC_L}{dt}v_L + \frac{dC_g}{dt}v_g = -\frac{k_{max}C_L X_a}{K_s + C_L}v_L$$

Separation of variables:

$$\frac{dC_L}{dt}v_L + \frac{dC_L v_g H_{cc}}{dt}v_g = -\frac{k_{max}C_L X_a}{K_s + C_L}v_L$$

$$\frac{dC_L}{dt}(v_g H_{cc} + v_L) = -\frac{k_{max}C_L X_a}{K_s + C_L}v_L$$

$$\frac{dC_L}{dt}(\frac{v_g H_{cc} + v_L}{v_L}) = -\frac{k_{max}C_L X_a}{K_s + C_L}$$

$$dC_L(\frac{K_s + C_L}{C_L X_a}) = -dt\frac{k_{max}V_L}{V_L + V_g H_{cc}}$$

Therefore:

$$k_{max,app} = \frac{k_{max}V_L}{V_L + V_g H_{cc}}$$

A6. Parameters input into the previously derived equation for best fit kinetic

parameters for suspended and immobilized methanotrophic cultures.

Table 6. Parameter ranges for integrated Monod model described in the Methods section.
Ranges indicated parameters input for both OB3b and 5GB1 cultures to fit experimental
parameter values. The *K* and μ_{max} values were fit to the experimental data using Excel Solver.

Integrated Monod Model			
Parameter	**Value Range**	**Units**	**Description**
S_s	0 - 0.0015	(mg CH$_4$/mL)	Liquid Phase Substrate Concentration
t	0 - 40	(hr)	Time
K_{max}	0.0089 - 0.0093	(mg CH$_4$/mg protein/min)	Max Specific Rate of Sub Utilization
X_f	0.42,0.52,1.46,1.62	(mg protein/mL)	Concentration of Active Protein
K_s	0.0019 - 0.0034	(mg CH$_4$/mL)	Half-Saturation Coefficient
Y	0.01-1	(mg protein/mg CH$_4$)	Cell Yield Coefficient

A7. Methane consumption data for 5GB1 and OB3b both suspended and

immobilized. Batch testing results from the integrated Monod experiment shown in

Figures 33 and *34.* Methane consumption was measured at two protein concentrations

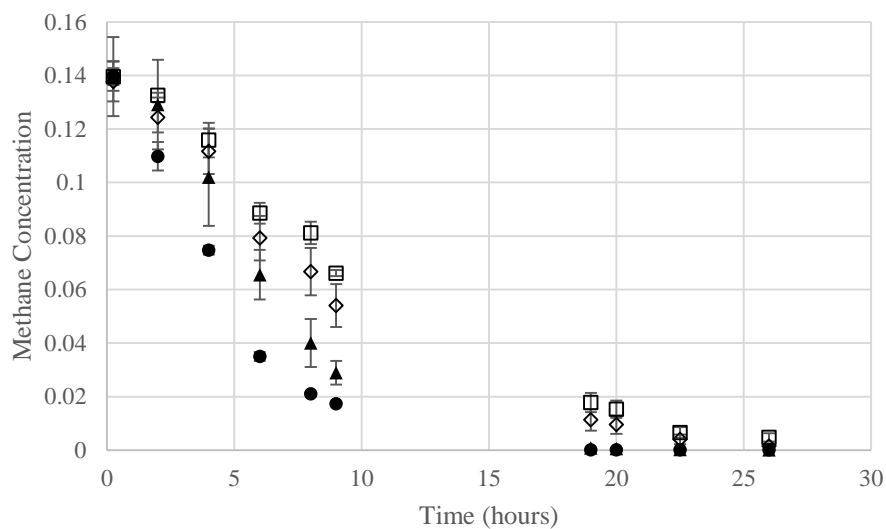for immobilized and suspended cultures for both 5GB1 and OB3b.

Figure 33. Methane consumption for suspended OB3b at 1.62 mg protein/mL (●),
immobilized OB3b at 1.62 mg protein/mL (◊), suspended OB3b at 0.52 mg protein/mL (▲),
and immobilized OB3b at 0.52 mg protein/mL (□). Points are averages with standard
deviation error bars from triplicate measurements. Conducted for integrated Monod
experiment.

Figure 34. Methane consumption for suspended 5GB1 at 1.46 mg protein/mL (●), immobilized 5GB1 at 1.46 mg protein/mL (◊), suspended 5GB1 at 0.42 mg protein/mL (▲), and immobilized 5GB1 at 0.42 mg protein/mL (□). Points are averages with standard deviation error bars from triplicate measurements. Conducted for integrated Monod experiment.
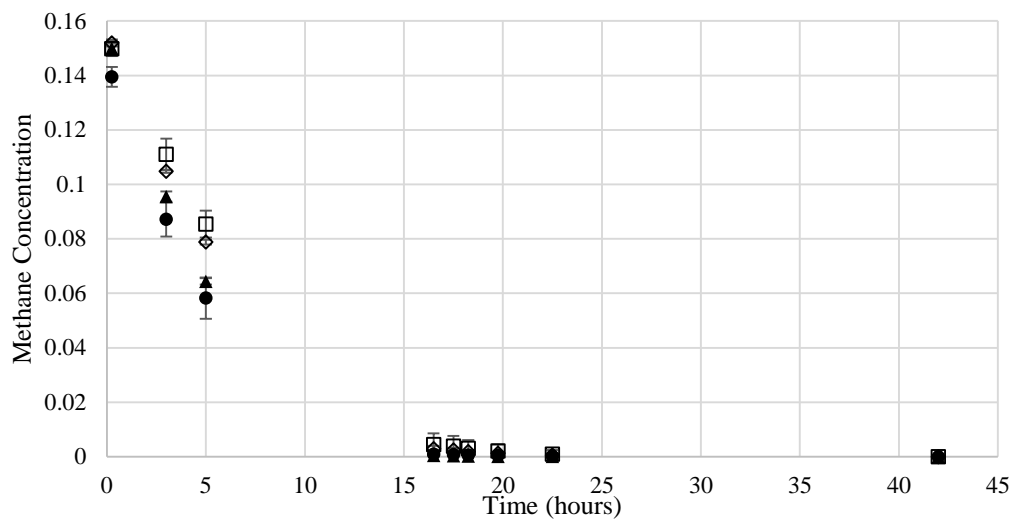
A8. Derivation of the biofilm kinetic-diffusion model for 3 CMBRs in series. The derivation goes a little more in depth of the process used to develop the model.

Derivation of 3 CMBR reaction-diffusion model into an active biofilm.

Substrate utilization in film:

$$r_{ut} = -\frac{\hat{q}X_f S_f}{K+S_f} \tag{39}$$

Molecular diffusion into film:

$$r_{diff} = D_f \frac{d^2 S_f}{dz^2} \tag{40}$$

Diffusion and utilization occur at the same time in the biofilm, so at steady state there is no accumulation and the overall utilization is:

$$0 = D_f \frac{d^2 S_f}{dz^2} - \frac{\hat{q}X_f S_f}{K+S_f} \tag{41}$$

Boundary condition 1: There is no flux beyond the film (at the base)

$$\left.\frac{dS_f}{dz}\right|_{z=L_f} = 0 \tag{42}$$

Boundary condition 2: External mass transport occurs according to Fick's First Law at the biofilm/media interface

$$J = \frac{D}{L}(S - S_s) = D_f \left.\frac{dS_f}{dz}\right|_{z=0} = D \left.\frac{dS}{dz}\right|_{z=0} \tag{43}$$

Equation 41 is analytically solved using the boundary conditions for the resulting flux equation into the biofilm (including reaction):

$$J = \left\{ 2\hat{q}X_f D_f \left(S_s + K ln\left(\frac{K}{K+S_s}\right) \right) \right\}^{1/2} \tag{44}$$

This equation is used for the mass transport into a biofilm located in a CMBR. A total mass balance on a CMBR is shown below:

$$0 = hV\frac{dS}{dt} = Q(S_0 - S) - J_{ss}aV \tag{45}$$

Solving for effluent substrate concentration:

$$Q(S_0 - S) = J_{ss}aV \tag{46}$$

$$(S_0 - S) = \frac{J_{ss}aV}{Q} \tag{47}$$

Final balance:

$$S = S_0 - \frac{J_{ss}aV}{Q} \tag{48}$$

$$S = S_0 - \frac{\left\{2\hat{q}X_f D_f\left(S_s + K\ln\left(\frac{K}{K+S_s}\right)\right)\right\}^{1/2} aV}{Q} \tag{49}$$

All parameters are known, and can be input analytically to solve for the effluent substrate concentration, and in turn the methane conversion.

Excel Solver Method:

The following method was used to directly calculate the model outputs shown in all performance comparisons.

A1	B1	C1	D1	E1	F1	G1	H1	I1
Residence Time (min)	Flow Rate (mL/min)	J_R for CMBR#1	S_{eff} for CMBR#1	J_R for CMBR#2	S_{eff} for CMBR#2	J_R for CMBR#3	S_{eff} for CMBR#3	Conversion

A set range of conversions were selected ranging from 0-1 with increments of 0.05. Using the initial substrate concentration and substrate conversion, the final effluent concentration from CMBR#3 is solved for:

$$\mathbf{H1} = S_0 - (\mathbf{I1} * S_0)$$

The flux in CMBR#3 is then calculated using the substrate concentration from H1 and *Equation 44*:

$$J = \left\{ 2K_{max}X_f D_f \left(S_s + Kln\left(\frac{K_S}{K+S_S}\right)\right)\right\}^{1/2} \tag{44}$$

$$\mathbf{G1} = \left\{ 2K_{max}X_f D_f \left(\mathbf{H1} + Kln\left(\frac{K_S}{K+S_S}\right)\right)\right\}^{1/2}$$

The flux from CMBR#3 is then used to back calculate the influent substrate concentration into CMBR#3 which is equal to the effluent substrate concentration from CMBR#2 (using *Equation 48*):

$$\mathbf{F1} = S_{eff,CMBR\#2} = S_{inf,CMBR\#3} = \mathbf{H1} + \frac{\mathbf{G1}\,aV}{Q}$$

Then the process is repeated to calculate the substrate concentrations and fluxes for all of the CMBRs:

$$\mathbf{E1} = \left\{ 2K_{max}X_f D_f \left(\mathbf{F1} + Kln\left(\frac{K_S}{K+S_S}\right)\right)\right\}^{1/2}$$

$$\mathbf{D1} = S_{eff,CMBR\#1} = S_{inf,CMBR\#2} = \mathbf{F1} + \frac{\mathbf{E1}\,aV}{Q}$$

$$\mathbf{C1} = \left\{ 2K_{max}X_f D_f \left(\mathbf{D1} + Kln\left(\frac{K_S}{K+S_S}\right)\right)\right\}^{1/2}$$

$$S_0 = S_{inf,CMBR\#1} = \mathbf{D1} + \frac{\mathbf{C1}\,aV}{Q}$$

All of the equations are dependent on the flow rate through the column, so Excel Solver was used to solve for the best fit Q (Excel Cell **B1**) to solve for the accurate influent substrate concentration S_0 using the least sum of squared error linear

regression technique. This flow rate was then used to calculate the residence time

through the column using the measured void volume:

$$\tau = \mathbf{A1} = \frac{\epsilon}{\mathbf{B1}}$$

This process was repeated for all conversions ranging from 0 to 1 in

increments of 0.05 for all protein concentrations for OB3b and 5GB1. This final

residence time is plotted against the conversion initially selected.

A9. Methane consumption values for the sequencing batch reactor experiment.

Methane measurements for initial and final methane totals in the batch reactors shown

in *Figure 35.* Points represent averages from triplicate measurements and error bars

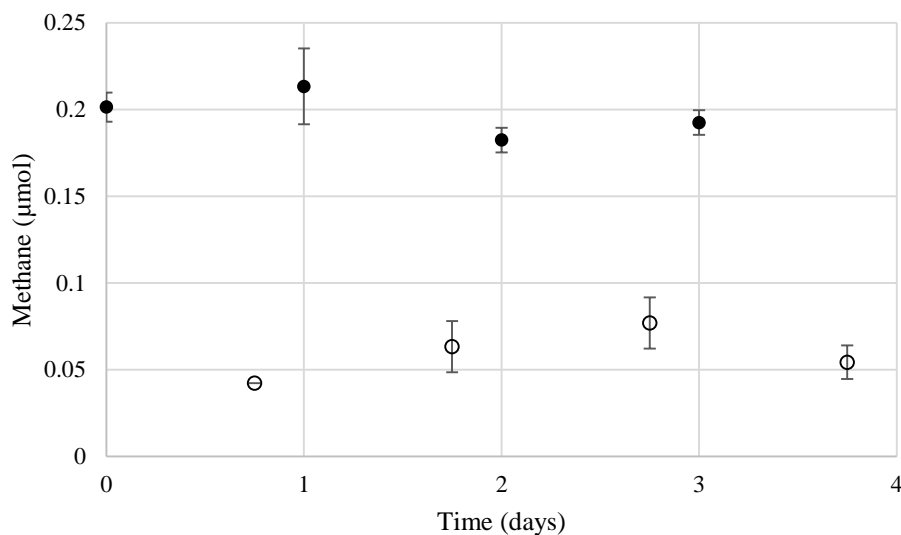are the standard deviation of the triplicates.

Figure 35. Sequencing batch reactor methane removal, measurements taken after methane is injected and again before beads are rinsed. Initial methane (●) and final methane (○) as a function of time. Methane consumption remains constant throughout the entirety of the methanol production phase.

A10. A transport test was conducted to measure the retardation of methanol transport through the column. Retarded transport would results from methanol sorption in the gel beads. This would also indicate that methanol may be leaching out of the alginate beads at a slow rate. A syringe of diluted methanol was passed through the column followed by fresh media to flush the methanol through. GC injections were used to measure methanol concentration for the duration of the experiment. Methanol concentrations measured in the effluent on the column are shown in *Figure 36.* The column was flushed with the fresh media at the point indicated by the dashed vertical line.
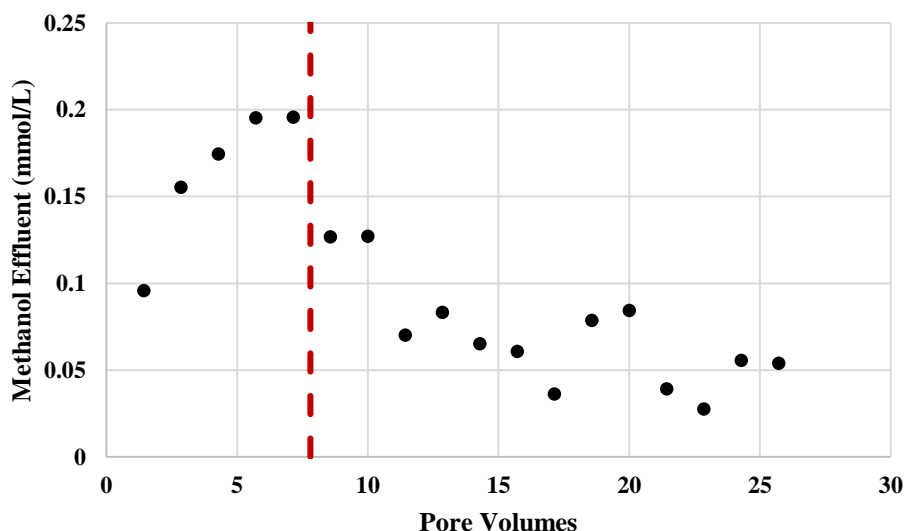

Figure 36. Methanol concentrations as a function of time. Flushing with fresh media began at the dashed line.

The buildup of methanol concentration over a period of 6 pore volumes indicated that the methanol sorption in the gel was occurring. The slow leaching of the methanol indicates that the methanol slowly diffuse out of the gel beads. Significant retardation of methanol was indicated.

A11. Explanation of parameter determination for the CMBR model.

The protein concentration is measured using a protein assay at the beginning of each experiment. The specific area is calculate based on the surface area of the biofilm and the total volume. For the gel beads, the surface area was estimated by the following equations:

$$Number\ of\ Beads = \frac{Total\ Gel\ Volume}{Volume\ of\ 1\ Bead}$$

$$Total\ Surface\ Area =\ Number\ of\ Beads * Surface\ Area\ of\ 1\ Bead$$

$$a = \frac{surface\ area}{volume}$$

The influent and effluent substrate concentrations were measured using liquid samples on the GC. The kinetic parameters (K_{max} and K_s) were determined for a batch suspended culture using Monod kinetics. The diffusion coefficient is an estimate using 80% of the diffusion coefficient of methane into water.

Table 7. List of parameters, values, units, and descriptions for the 3 CMBR model. Ranges indicate experimental variability and variations between OB3b and 5GB1. Discussion of parameter determination in the appendix.

Parameter	5GB1 Values	OB3b Values	Units	Description
X_f	0.9-6.6	3.1-18	(mg protein/mL bead)	Concentration of active protein
a	15	10	(cm^2/cm^3)	Specific surface area
S_0	7.2-7.9	7.2-7.9	(mg CH_4/mL)	Inlet liquid phase substrate concentration
K_{max}	0.0093	0.0089	(mg CH_4/mg protein/min)	Maximum specific rate of substrate utilization
D_f	0.001	0.001	(cm^2/min)	Diffusion coefficient
K_s	0.0019	0.0023	(mg CH_4/mL)	Half-saturation coefficient
ε	5-7	9-10	(mL)	Void Volume

A12. Base case and BLP parameters for the CMBR model evaluation. Specific area

of the BLP model determined from the thin film dimensions described below.

Gel Surface Area: 267.5 cm^2

Gel Volume: 13.34 cm^3

Void Volume: 13.49 cm^3

Table 8. Base case and BLP parameter inputs for the CMBR model performance comparison.

Parameter	Base Case	BLP Case	Units
X_f	5	5	(mg protein/mL bead)
a	11	20	(cm^2/cm^3)
S_0	7.7	14	(mg CH$_4$/mL)
K_{max}	0.0093	0.0093	(mg CH$_4$/mg protein/min)
D_f	0.001	0.001	(cm^2/min)
K_s	0.0019	0.0019	(mg CH$_4$/mL)